



AGH

**AKADEMIA GÓRNICZO-HUTNICZA IM. STANISŁAWA STASZICA W KRAKOWIE
OF FUELS ENERGY AND FUELS**

Thesis project

*GIS-based approach for local energy planning
Lokalne planowanie energetyczne z wykorzystaniem
narzędzi GIS*

Author: *Aravind Satish*
Field of study: *Sustainable Energy Systems*
Supervisor: *Dr hab. inż. Artur Wyrwa, prof. AGH*

Krakow, 2021

Table of Contents

Abbreviations.....	4
Important Terms	5
1 Introduction.....	6
1.1 Research Questions, Goals and Scope.....	6
2 Literature Review	8
2.1 Mapping urban heat demands.....	8
2.2 GIS assisted mapping of urban heat demand.....	10
2.3 Energy-demand reduction through retrofitting of residential homes	11
2.4 GIS based estimation of solar PV rooftop potential.....	12
3 Softwares.....	18
4 Methodology	21
4.1 Estimating rooftop solar PV potential and power production.....	21
4.1.1 Method 1: estimating solar PV output using regression model of solar radiation using data from PVGIS.....	22
4.1.2 Method 2: estimating solar PV output using solar radiation model of SAGA GIS	25
4.2 City-level energy planning using urban heat demand model	29
4.2.1 Defining global sets	32
4.2.2 Building representation.....	33
4.2.3 Decision variable.....	33
4.2.4 Equations.....	33
4.3 Financial assessment of rooftop solar PV instalments.....	35
5 Results.....	37
5.1 Rooftop solar PV output.....	37
5.2 Energy system modelling—deciding retrofitting measures.....	39
5.2.1 Without rooftop solar PV	40

5.2.2	With rooftop solar PV	45
6	Business model for accelerating rooftop PV installation	47
7	Conclusions	51
8	Nomenclature.....	53
9	References	54
	Appendix I.....	59
	Appendix II.....	60

Abbreviations

PM	Particulate matter
EU	European Union
UN	United Nations
SDG	Sustainable Development Goals
DSM	Digital Surface Model
SEBE	Solar Energy on Building Models
DEM	Digital Elevation Model
WRDC	World Radiation Data Centre
PVGIS	Photovoltaic Geographic Information System
SEBE	Solar Energy on Building Envelopes
GRASS	Geographic Resources Analysis Support System
BES	Building Energy Simulation
MILP	Mixed Integer Linear Programming
GAMS	General Algebraic Modelling Systems
NPV	Net Present Value
PPA	Power Purchase Agreement
BMC	Business Model Canvas

Important Terms

Vector layer	A data structure that is used for storing spatial data. It is composed of lines or arcs, each of which is defined by beginning and end points. These points usually meet at 'nodes'. The locations of these nodes and the topological structure are usually stored explicitly. The features in a vector file are defined only by their boundaries.
Raster layer	A data structure that represents geographic features splitting the globe into discrete cells that are square or rectangular shaped. These cells are spread on a 'grid'. Every cells carries data within it such as elevation, temperature, location, etc.
Shapefile	A nontopological format for storing the geometric location and attribute information of geographic features by using points, lines, or polygons (areas).
Attribute table	Each vector layer has a corresponding attribute table with each vector data has a corresponding row in the attribute table, which contains the non-spatial information about it.

1 Introduction

Drastic and prolonged exposure to air pollution has been associated with severe health effects (Peters *et al.*, 2000). Millions of people die every year due to air pollution and about 2.1 of it can be attributed to particulate matter (PM) (Kim, Kabir and Kabir, 2015). The health effects include premature death among people with heart or lung disease, nonfatal heart attacks, irregular heartbeat, aggravated asthma, decreased lung function, and increased respiratory symptoms such as irritation of the airways, coughing, or difficulty breathing (Kim, Kabir and Kabir, 2015).

Poland has one of the worst air qualities in the EU during winter due to low-stack emissions borne from burning solid fuels such as coal in boilers for central heating. This releases particulate matter and hazardous materials like Mercury into the atmosphere (Wyrwa, 2019). Besides PM, the combustion of solid fuels also releases tons of greenhouse-gases into the atmosphere every year.

Poland's buildings experienced development at different stages and different districts have been developed differently at different time periods (Wyrwa and Chen, 2017). Therefore, not all buildings may be performing at its best in terms of (heating) energy efficiency. The energy losses incurred due to faulty equipment, outdated technology or improper building-insulation can result in high energy consumption.

This calls for a roadmap for pollution abatement and heat-demand reduction in Poland; a roadmap that will delineate benchmarks for sustainability. Doing so is a step towards recognizing Sustainable Development Goals (SDGs) 3 (good health and well-being), 7 (affordable and clean energy), 11 (sustainable cities and communities), 12 (responsible consumption and production) and 13 (climate action) as elaborated by United Nations (UN).

1.1 Research Questions, Goals and Scope

The present study is confined to the town of Kalwaria Zebrzydowska. It is a town in southern Poland with 4,429 inhabitants (2007 estimate). It has an area of about 5.5 km² and a population density of 820/km². The inception of this

project began with the following questions with respect to Kalwaria Zebrzydowska and therefore the current research is aimed at addressing them:

- What is the current state of the types of space and water heating in Kalwaria in terms of technology and the fuels used for heating?
- What is the state of each household in Kalwaria in terms of wall-insulation, window-types, roof insulation, etc. and can they be categorized into different classes of a building stock¹?
- Are there any scopes for upgradation of the existing building state to achieve higher energy efficiency and lower CO₂ emissions?
- Can Kalwaria be made more sustainable with rooftop solar PV installations?
- How much will the upgradations cost?

The goal of this study is to identify methods and formulate recommendations to reduce Kalwaria's heating needs and parallelly it's air pollution. It will also estimate the amount of solar PV energy that can be generated in Kalwaria using a solar cadastre. Not only are the recommendations expected to help the town and its people realize SDGs, they will also help build a model for the development of future Polish towns and cities.

¹ buildings are categorised based on their functionality and period of construction. Each building category or stock has a representative building with its characteristics noted in detail. These representative buildings are then used to map the heat demand for the entire region.

2 Literature Review

2.1 Mapping urban heat demands

The building-stock concept is very popular in urban heat demand mapping. This concept was used by Wyrwa and Chen, 2017, to estimate the amount and type of thermo-modernization required in the city of Krakow. Wyrwa and Chen, 2017, describes a method to estimate short-term and long-term energy demands of buildings in Krakow, Poland. This required the analyses of the energy demand of the past, present and future for space-heating and domestic hot water. Therefore, short-term demand projections were estimated using information about buildings that were under construction and those that were scheduled to be constructed in the next 3 years. Long-term demands were analysed with the help of building stock models and projections up to 15 years. The geo-referenced data used to inspect and categorize the buildings were building boundaries, number of floors, types of utilities used in the building, intensity of energy consumption in the building and boundaries of the city or district to help visualize the results.

The building stock data can be obtained from the national building typologies developed under TABULA project (IEE Project TABULA, 2012) where residential buildings were categorized based on their functions and construction periods. Building stock data can also be obtained from National Energy Performance Building Databases (EPBD). The EPBD database was used by Mahmoud *et al.*, 2019, to create load duration curves of with the help of building energy simulation (BES) models.

Load duration curves can help estimate the heating and cooling demands of households with higher accuracy. This avoids oversizing of heating and cooling installations and higher design costs required for time consuming dynamic simulations that would have been needed to size utility systems without using load duration curves (Mahmoud *et al.*, 2019). The load duration curves were developed through 6 steps—(1) accumulating general building data (such as geometry of the building, physical properties of the building, gross floor area, volume, average heat-transfer coefficient of the windows and buildings envelopes) of the building stock (2) identifying the archetype that represents a specific building typology (3) performing geometric fitting to fit the one-

dimensional form of the building (from the building stock) to a three-dimensional form, which is also the archetype (4) gathering the physical parameters of the building such as heat-transfer coefficient of the building envelop, occupancy, window properties, orientation of the building, etc. (5) making a BES model using these parameters (6) simulating the heating and cooling demands to create the load duration curves.

One of the methods to calculate the heat demand of each building is explained in Wyrwa and Chen, 2017. The total heated area of each building was required and they were calculated using the following equation (Wyrwa and Chen, 2017). Nomenclatures, subscripts, and superscripts have been listed under section 8.

$$A_b^f = A_b^z \cdot l \cdot c_b^f \quad \forall b \in B [m^2] \quad (2.1)$$

Based on this area, the useful heat demand for each building and energy service was calculated using the following equation (Wyrwa and Chen, 2017).

$$Q_b^u = A_b^f \cdot e_{s,t}^u \quad \forall b \in S \cap T [kWh/year] \quad (2.2)$$

Table 3.1 shows heated area calibration ratio (c^f) and specific heat demand (e^u) used in equations 1 and 2 (Wyrwa and Chen, 2017).

Table 2.1: Coefficients of residential buildings used in this case study

Building type	c^f [-]	Specific heat demand [kWh/(m².year)]	
One-family house	0.79	e^{h1}	184.1
		e^{ve}	57.07
		e^w	24.09
Two-family house	0.76	e^{h1}	162.15
		e^{ve}	62.38
		e^w	27.53
Multi-family house	0.79	e^{h1}	274.15
		e^{ve}	41.22
		e^w	27.53
Collective building	0.8	e^{h1}	88.45
		e^{ve}	44.52
		e^w	43.01

Source: (Wyrwa and Chen, 2017)

The total energy demand can be obtained by adding the energy used for space-heating, hot water and ventilation as shown in equation 2.3.

$$\sum Q^u = Q^{h1} + Q^{ve} + Q^w \quad (2.3)$$

2.2 GIS assisted mapping of urban heat demand

It was clear that the buildings' envelop was important in deciding its energy behaviour. Theodoridou *et al.*, 2012, delineated a method to determine the average horizontal and vertical surface areas using building geometry obtained from GIS tools. It also explains how to translate this knowledge into the required retrofit measures and the costs that would be incurred upon retrofitting the building. The type of retrofitting or energy intervention depends on the available vertical and horizontal surfaces. It is also influenced by the area of opaque surfaces exposed to the outside and the wall-to-opening ratios (Theodoridou *et al.*, 2012). The net building surface area (or the opaque building surface area) is the difference between the wall area and the area of windows. Inspecting each building facade for the available opaque surface area would be time consuming; hence the GIS buildings were matched with data available for sample buildings from the building stock.

It was also identified that the ratio of the total building's envelop surface (A) to its conditioned volume (V) is very instrumental in associating the energy-behaviour of the building with its structure (Theodoridou *et al.*, 2012). Greater is the exposed surface (or A/V ratio), higher is the energy loss.

Mastrucci *et al.*, 2014, explained a GIS-based bottom-up approach combined with statistical methods to estimate the energy demand in residential building stocks. The bottom-up study uses a hierarchy of disaggregated input data to extrapolate the data, using statistical means, to find the energy demand of the building-stock. For the statistical assessment, results of regression analysis, decision tree and neural networks were assessed and found to be comparable. However, a regression-equation was preferred to identify the parameters/variables used for calculating the energy demand. A regression-equation was formulated to downscale the natural-gas and electricity consumption from zip-code level to individual households using variables related

to housing characteristics. And ordinary least-square regression was used to fit the data. The statistical model was also validated using boot-strapping.

2.3 Energy-demand reduction through retrofitting of residential homes

In light of the extant requirement of sustainability, architectural designs try to balance all the physical performance of buildings as much as possible; and the balance can be checked by simulating the selected design choices. However, traditionally/earlier, this process used the work-flow of “design simulation—design modification” which is time and resource consuming. Shi, 2011, endorses the use of optimisation tools to improve the efficiency of the existing simulation algorithms through because the combined optimisation-simulation routine can automatically generate design strategies to search for the best choice. Shi, 2011, demonstrates this using an office building in Nanjing, China where EnergyPlus program was integrated into the optimization tool to explore the best insulation scheme to reduce space conditioning.

Anastaselos, Oxizidis and Papadopoulos, 2011, demonstrated a novel decision support system to assess the performance, also, of thermal insulation solutions and applied it to energy conservation to multi-family homes in Greece. The assessment included 3 factors that encompasses the life cycle of the insulation strategy: primary energy consumption, environmental impact and its costs. It led to the creation of a all-inclusive decision support tool called ib3at.

Modification of roofs can also be offered as solutions to minimize energy demand. Fioretti *et al.*, 2010, discusses the impact of energy and water (mass) fluxes on vegetated roofs specific to the Mediterranean region. Vegetated roofs were found to outdo non-vegetated roof in attenuating solar radiation and retain water during storms which also helps to reduce inside-temperatures.

In Wyrwa, 2019, the retrofit measures examined were window replacement, thermo-modernisation of outer walls, roof insulation and replacement/ modernisation of central heating. A model was made to choose between these retrofit measures to obtain the least expensive building configuration (by estimating the CAPEX and OPEX) that would meet the energy demands. The model also allowed for setting constraints on the emissions and

budget allowed. The model was built in the General Algebraic Modelling System or GAMS. The details of this model will be further elaborated in the Methodology section since the model was adapted into this project.

Evidently, by integrating a wide variety of energy saving techniques and diverse technologies, urban energy demands can be met in a cost effective way. Jing *et al.*, 2020, quantified the contribution of individual strategies. The method also used Mixed Integer Linear Programming (MILP). The contribution analysed was the system value of each technology. Jing *et al.*, 2020 defined the system value as the reduction in system cost in a solution obtained from an optimisation model, in comparison to a benchmark, by progressively increasing the presence of the technology that was being examined. The objective function of the optimisation model was the sum of the OPEX and annualised CAPEX; the benefit or the magnitude of the system value was the reduction in OPEX plus the reduction of CAPEX due to the change in the availability of the technology's being evaluated.

2.4 GIS based estimation of solar PV rooftop potential

Rooftop solar PV installations have the advantage of being a democratic source of energy—anyone can have access to and use solar energy. They also allow for on-site clean energy generation, assist in decarbonizing the energy sector and is also one of the renewable energy technologies that help to establish nearly-zero-emission-buildings. Moreover, with the efficiencies of solar panels increasing and their production costs decreasing, investments in solar photovoltaics will become more lucrative with each passing day. The sheer amount of area available atop the infinite number of extant buildings—commercial or residential, concrete or wood, single-story or multi-story, points to a vast opportunity for harvesting solar energy which is either untapped or under-exploited.

Nevertheless, rooftops suitable for solar PVs are not ubiquitous. Shadows cast by overhead vegetation and adjacent buildings, presence of chimneys and dormers and roofs angles unfavourable to receiving abundant solar radiation are a few of the factors that need to be considered for selecting solar-suitable-areas.

On-line solar cadastre services such as SoDa (Solar radiation Data), SOLEMI (SOLar Energy Mining) and PVGIS provide researchers with solar irradiance

maps that accelerate the identification and study of solar-suitable-areas. Compared to traditional approaches, GIS based approaches are more cost effective and time conserving. Solar cadastres can also be created instead of retrieving them from the internet for obtaining maps that are better calibrated to a project's requirement (such as higher map resolution).

Agugiaro *et al.*, 2012, explains how to generate solar cadastres of building roofs in complex Alpine landscapes. Among the main tasks, Agugiaro *et al.*, 2012 attempted to create high resolution Digital Surface Models (DSM) of the roof tops. The study used high resolution geometric models of the buildings using automated image matching techniques using photogrammetric point clouds to create the DSMs. DSMs were also created using LiDAR data. Both models incorporated atmospheric effects, terrain characteristics, chimneys, dormers, vegetation covers, adjacent buildings and geographical site position and elevations. The solar cadastre was finally generated using the *r.sun* and *r.horizon* tool of the software GRASS after calibrating it with the appropriate meteorological data. Results obtained from both sources were compared.

Besides adjacent buildings, vegetation-covers also significantly affects shadow patterns. Lindberg *et al.*, 2015, developed a new model for calculating shortwave irradiation on the grounds, building walls and roofs. The model is called Solar Energy on Building Models (SEBE) and it uses 2D DSMs to obtain 3D solar cadastres. The model requires a high-resolution ground-and-building DSM as an input to avoid offsetting the walls due to coarse pixel resolution. The models also reads a wall-height raster (which documented the height of the boundaries/envelops of the buildings in each pixel) and an aspect raster (which documents the direction of the slope present in each pixel) as inputs. Most importantly, two vegetation DSMs—the canopy height and the trunk-zone height are also read as inputs. The canopy DSM describes height of the trees/top of the vegetation and the trunk-zone DSM describes the height of the base of that canopy.

The SEBE model has undergone many modifications and the new algorithm is able to create 'shadow volumes' DMS separately for the vegetation raster-layers. Shadow volumes are created by moving the DSM at the azimuth angle of the sun sequentially, while the height is reduced iteratively on the basis

of the sun's elevation angle. There is also an algorithm in place to retrieve the sunlit parts of the building-walls using edge-detection filters as a means to identify pixels representing walls.

The SEBE model is also fed with hourly meteorological data. The objective of the meteorological data is to calculate the direct shortwave radiation component on a surface perpendicular to the sun. A database which delivers the magnitudes of the shortwave component is desirable. Otherwise it is calculated using values of diffuse radiation on the surface which in turn can be calculated from global irradiation data (Lindberg *et al.*, 2015).

Another tool for the estimation of solar insolation is the *Potential Incoming Solar Radiation* tool of SAGA (System for Automated Geoscientific Analyses) GIS environment and has been demonstrated by Luković *et al.*, 2015, to analyse the solar insolation in Serbia. The methodology implemented in SAGA for estimating solar insolation uses three broad governing factors—(1) the Earth's orientation relative to the sun, (2) clouds and other atmospheric inhomogeneities and (3) topography (Böhner and AntoniĆ, 2009). SAGA GIS reads a Digital Elevation Model (DEM) as input and it derives slope, aspect, local sky-view-factor, shadows and geographical coordinates from the DEM. To process atmospheric inhomogeneities, additional cloud-cover data has to be provided; however, empirical values can also be used such as lumped atmospheric transmittance (in units of percentage).

The net solar radiation (R_n) at a place is the sum of the long-wave (L_n) and short-wave radiation (S_n) received locally.

$$R_n = S_n + L_n \quad (2.4)$$

The most relevant component, S_n , is composed of direct solar radiation (S_s), diffuse solar radiation (S_h), the radiation received after it has bounced off from surrounding land surfaces (S_t) and derived of the radiation reflected away from the surface (S_r).

$$S_n = S_s + S_h + S_t - S_r = (S_s + S_h + S_t) \times (1 - r) \quad (2.5)$$

Where r is the surface albedo.

If it was assumed that S_n refers to the irradiance on a horizontal surface unobstructed by surrounding features (in lieu of a realistic surface with a non-

zero slope and aspect) and S_s , S_h and S_t also correspond to a horizontal plane, $S_t=0$. Let S_n^* , S_s^* and S_h^* be the values of radiation when topographical features are accounted for. Then, according to Böhner and AntoniĆ, 2009,

$$S_{s(h)}^* = \zeta \cdot \frac{S_{s(h)}}{\sin\theta} \cdot \cos\gamma$$

Where, $S_{s(h)}^*$ is the hourly direct solar radiation, ζ is the shadow binary variable (0 when shadowed and 1 otherwise), θ is the elevation angle of the sun, γ is the solar illumination angle. Daily direct solar radiation is calculated by adding the hourly direct solar radiation of the day. S_h or the diffuse irradiance is a function of solar geometry, pressure (elevation), scattering and absorbing properties of the atmosphere and the sky view factor, Ψ_s . The sky view factor is given by (Böhner and AntoniĆ, 2009):

$$\Psi_s = \frac{1}{2\pi} \int_0^{2\pi} [\cos\beta \cdot \cos^2\varphi + \sin\beta \cdot \cos(\Phi - \alpha) \cdot (90 - \varphi - \sin\varphi \cdot \cos\varphi)] df \quad (2.6)$$

Where, Φ is the azimuth angle, φ is the corresponding zenith angle of the local horizon, α is the aspect of the surface and β is the slope of the slope of the surface. Then, S_h^* is defined as:

$$S_h^* = S_h \cdot \Psi_s \quad (2.7)$$

The above algorithm is implemented in the *Potential Incoming Solar Radiation* tool of SAGA GIS.

According to Kereush and Perovych, 2017, typically photovoltaic systems require a minimum of 1100 kWh/m² of radiation per year to be economical. Furthermore, steep roof slopes make the construction of the PV system difficult due to factors related to drainage, erosion, and the stability of the foundation; this will increase costs of installation. The maximum slope for a suitable roof should be 15° (Kereush and Perovych, 2017). Ideally the panels should also operate in conditions where the air temperature is 15-40°C to maintain.

So far, the physical and geographical potentials solar PV generation was discussed/accounted for. Physical potential refers to the total solar radiation on the roof tops and geographic potential concerns the available solar radiation

after shadowing is analysed. Further there is also a need for an analysis of the technical potential—electricity generation considering solar PV module size (to check if the panels fit on the roof) and module efficiency. Hong *et al.*, 2017, demonstrated a process of filtering out the technical potential of rooftop solar PV through a Hillshade analysis of the rooftops in Gangnam district in Seoul South Korea.

Hong *et al.*, 2017, estimated the physical potential with the help of hourly solar radiation data available to the public from World Radiation Data Centre (WRDC). The geographic potential was estimated in three steps: (1) a DEM was created or obtained where elevation-data of buildings is available and all elevation of other features (ground and areas without buildings) are set to 0, (2) hillshade analysis of the buildings was performed to identify shadowed areas; hillshade analysis required the previously created DEM, altitude of the sun above the horizon and the sun's azimuth. The hillshade analysis was performed for 12 days of the year (15th of every month for an average day of the month) for every hour between 6 am and 7 pm, creating 156 raster layers showing the shadowed areas of the buildings. Finally (3) the unsuitable (completely dark/shadowed) areas were excluded from the selection of rooftops.

To determine the technical potential of rooftop solar PVs, the number of solar modules that can be fitted on the rooftops were identified using data of the minimum area required for a standard solar PV system corresponding to 1 kW. Further, an efficiency of 15 % was assumed for the solar panels to estimate the maximum electricity that can be generated (Hong *et al.*, 2017). 156 raster layers were filtered according to the above algorithm and monthly profiles of physical, geographic and technical potential was analysed.

Analyses of the technical potential was also performed by Šúri *et al.*, 2007, however on a much larger scale. The work explored the expected annual electricity generation from a standard 1 kWp grid connected solar PV system in 25 European member states and 5 candidate countries, in a project designed to create an opensource, high resolution, easily comprehensible database. The solar radiation database was created using the solar radiation model *r.sun* which is one of the tools in GRASS software as mentioned before. The spatial resolution of the output grid-layers was 1 km x 1 km and contained 12 monthly

averages for the years 1981-1990 constituting data of daily global irradiation on horizontal surfaces, ratio of diffuse to global horizontal radiation and clear-sky index. This database was called Photovoltaic Geographic Information System or PVGIS.

Šúri *et al.*, 2007, used the PVGIS database to estimate the potential electricity generation from solar PV systems kept at horizontal, vertical and optimal inclination using the following equation:


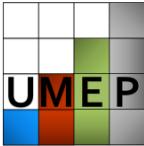

$$E = P_k \cdot PR \cdot G \quad (2.8)$$



Where, E is the annual total electricity generated (kWh), P_k is the unit peak power of the installed PV system (kW) and was assumed to be 1 in their calculations, PR is the performance ratio of the PV system and G is the yearly sum of global irradiation on a horizontal, vertical or inclined PV module (kWh/m²).

3 Softwares

For conducting the spatial analyses and optimisation routines required by this project, the following softwares were considered as potential candidates.

Table 3.1: Comparison of candidate softwares considered in this study

Software/Tools/Programs	Description
QGIS 	<p>Quantum GIS or QGIS is an open-source software that functions as a desktop GIS, permitting its users to investigate and alter spatial information and compose and export graphical maps. QGIS permits both raster and vector layers. QGIS combines other open-source GIS packages such as PostGIS, GRASS GIS, SAGA GIS, Kosmo and MapServer. Plugins coded in Python or C++ can also be added to QGIS. QGIS can also be used with SAGA GIS and Kosmo.</p>
UMEP 	<p>Urban Multi-scale Environmental Predictor is an open-source climate service tool and is a part of QGIS. UMEP can be used for analysing outdoor thermal comfort, urban energy consumption, climate change, etc. UMEP also allows spatial analyses through viewing and editing of data. The Solar Energy on Building Envelopes or SEBE model, incorporated into UMEP, allows the computation of irradiance on ground surfaces, building roofs and walls. SEBE uses a shadow-casting algorithm to identify sunlit and shadowed areas at pixel level using a DSM.</p>
GRASS 	<p>Geographic Resources Analysis Support System or GRASS is also a GIS platform that supports viewing, editing and analyses of spatial data. It is an open-source software. Besides vector and raster data formats, GRASS can also work with 3D data formats (map algebra, visualisation and interpolation). GRASS contains more than 500 modules to process geographic data and can run simple to complicated analyses. Some important features include point-cloud analysis, temporal analysis, image processing and spatial</p>

	<p>statistics. The temporal analysis aids in the shadow analysis at different times during the day/month/year. QGIS provides a GRASS plugin, though, with limited features.</p>
<p>SAGA</p> 	<p>System for Automated Geoscientific Analyses is an open-source GIS software. SAGA provides simplified implementation of new algorithms for geographic data analyses and is, hence, an easily learnable platform. Standard modules in SAGA allows geostatistics, grid analyses (filters, calculators, discretisation), grid tools, cluster analyses, maximum likelihood analyses, pattern recognition, etc. Most interestingly it also allows terrain analyses which encompasses slope and aspect calculation, analytical hillshading and solar radiation-estimation among others.</p>
<p>GAMS</p> 	<p>The General Algebraic Modelling System or GAMS is an optimization platform designed for solving linear, nonlinear and mixed-integer optimization sums. GAMS was fabricated to solve complex and large-scale problems that can be easily modified for different scenarios.</p>

The spatial analyses required for the current project necessitates the use of vector-layers with linked attributes, selection of specific polygons on vector-layers, cutting-out/clipping raster-layers within specific polygons, raster-layer calculations, zonal statistics and slope and aspect derivations among many other functions. Being an open-source software and easily comprehensible software, QGIS was chosen as one of the platforms for this study. Furthermore, QGIS also includes extensions of GRASS, SAGA and UMEP within itself.

To create a solar cadastre, a 1 meter x 1 meter pixel-level solar radiation map showing the radiation received by all normal, horizontal and tilted surfaces on the DSM was to be generated. It was attempted to use the UMEP-SEBE plugin of QGIS with the help of solar radiation and meteorological data obtained from SoDa. However, due to the extremely long computational time required to run the program, the UMEP-SEBE plugin was not used. The *r.sun* tool of GRASS was not available on its extension available on QGIS to perform the routine

demonstrated by Agugiaro *et al.*, 2012; however, *r.sun.insoltime* tool was available. Solar irradiation modelling in GRASS provides more sophisticated and facilitates better tuning of input parameters. Nevertheless, the *Potential Incoming Solar Radiation* of SAGA was used to derive the solar radiation map because SAGA has a very user-friendly interface and the solar radiation computations are 2-3 times faster than the GRASS tools. And for the scope of this project, SAGA's features sufficed. Since the *Potential Incoming Solar Radiation* tool was not available on the SAGA extension provided on QGIS, it was decided to perform the solar irradiation modelling independently on SAGA version 7.9 and then import the results into QGIS for further processing.

The project also requires the use of an optimization system to identify the building configurations that would reduce the energy consumption and in turn the emission of air pollutants in the city of Kalwaria. GAMS was chosen as the optimisation system owing to:

- Simplicity of implementation
- Portability and transferability between users and systems
- Ease of collaboration of codes/ algorithms among users
- Time saved in entering data as it allows reading of data in list and table formats which can also be fed in .xlsx or .csv formats.
- Allowance of data conversion of inputs and (or) results from one format (eg. .xlsx) to another (eg. csv).

4 Methodology

This section explains the methods used to create the solar cadastre for the city of Kalwaria Zebrzydowska. Two methods were attempted and compared based on their accuracy of results. Further, this section also explains the method employed to identify the retrofitting measures ideal for reducing the heating demands and quantity of air-pollutants emitted due to the fuel consumption. Furthermore, the solar cadastre which was developed was also used to analyse the feasibility of installing rooftop solar panels in Kalwaria and identify on which buildings it is feasible.

4.1 Estimating rooftop solar PV potential and power production

This section explains the 2 methodologies used to estimate the rooftop solar PV potential in terms of the maximum power and the energy that can be generated from Kalwaria through the creation of a rooftop solar cadastre. For both methods, to design a solar cadastre of the city of Kalwaria, the first step was to create a project file in QGIS, which will be the main software used for viewing, editing and analysing spatial data. The Coordinate Reference System (CRS) was set for all further layers under project properties. The CRS was set to ETRS89/ Poland CS92-Projected since the area under concern was in Poland. The unit of grid measurement is meter. The following layers were necessary to perform the analyses:

- A shapefile for the city of Kalwaria. The shape file consisted of a single polygon where its perimeter represented the boundaries of the city of Kalwaria. This is represented by the purple region in Figure 4.1(a)
- A shapefile layer representing each residential building, within the shapefile of the city, in the form of polygons. Since the scope of this study is limited to residential one-family, two-family and multi-family houses, only they were included in the shapefile. This shape file is represented in the form of green polygons as shown in Figure. 4.1(b)
- A DSM-layer of the city of Kalwaria. A 1 meter x 1 meter resolution was chosen for the model. Further finer resolutions would increase the time of the analyses performed on the layer and coarser resolutions would make

these analyses less prices. The DSM prepared is presented in Figure 4.2 in greyscale. The DSM was obtained from <https://geoportal.gov.pl>

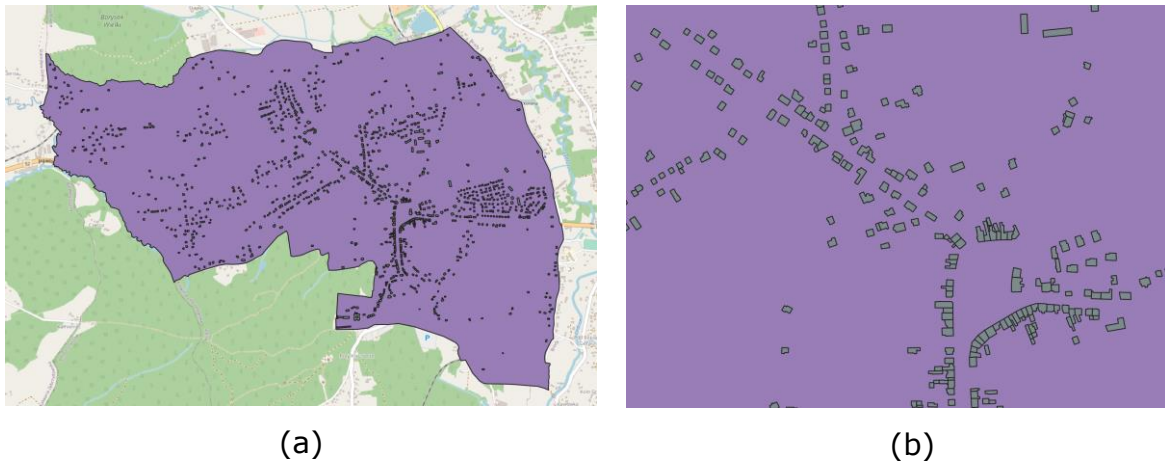
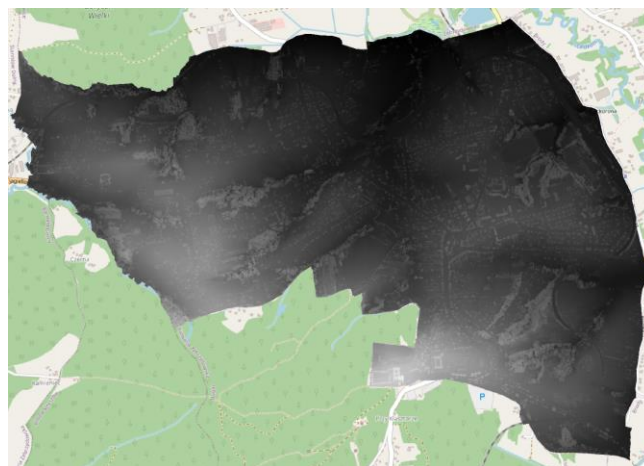


Figure 4.1: Shapefiles of (a) Kalwaria city (purple region) and the residential houses (green polygons) within (b) magnified image of the polygons representing the residential houses. [Source: own study]



[Source: own study]

Figure 4.2: DSM layer of Kalwaria City (shown in greyscale)

4.1.1 Method 1: estimating solar PV output using regression model of solar radiation using data from PVGIS

To estimate the solar energy that can be generated by rooftop solar PV installations yearly in-plane irradiation was required for the roof of each building. The yearly in-plane irradiation depends on the slope of the roof and its azimuth angle (among other factors). The azimuth and slope of the roofs of the buildings can be obtained using QGIS tools. The slopes of all surfaces on the DSM of

Kalawria city were obtained using the *Slope*² tool under *Raster Analysis* of QGIS. The *Slope* tool calculates the average angle of inclination, from the horizontal, of all the surfaces in each pixel. The slopes of only the residential buildings were isolated and extracted using the *clip raster by mask layer*³ tool of QGIS. Similarly, the azimuth of all the surfaces of the DSM of Kalwaria city was obtained using the *Aspect* tool under *Raster Analysis* and the aspect of the residential buildings were extracted using the *Clip raster by mask layer*.

Using the *Zonal Statistics* tool of QGIS it is possible to derive the average slope and azimuth of the roof of each building by calculating the average slope and azimuth of all the pixels comprising the roof. This will retrieve a single value for both the slope and azimuth of each roof. However, using a single azimuth and slope value for the whole roof of a building is bound to give erroneous results as different sides of a roof can face different direction. Therefore, for improving accuracy of calculation, each roof was divided into four parts. Note that, in QGIS, azimuth is measured from 0° to 360° in the clockwise direction starting from North which is at 0°.

Part 1 consisted of the North facing roofs which had azimuths of 0°-90°. Part 2 consisted of the East facing roofs which had azimuths of 90°-180°. Part 3 consisted of the South facing roofs which had azimuths of 180°-270°. And part 4 consisted of the West facing roofs which had azimuths of 270°-360°. Each part was isolated and extracted using the *Raster Calculator* tool. For example, to obtain part 1, QGIS was instructed to select pixels where the azimuth is only 0°-90°. Afterwards, the average values of the slope and azimuth for each part was calculated using *Raster Calculator* and *Zonal Statistics* tools. These values were later added into the attribute table of the vector layer (shown in Figure 4.1) describing the residential houses in Kalwaria. Shown below in Table 4.1 is an example of how the attribute table looked like:

² The slope tool calculates the average angle of inclination from the horizontal of all surfaces in each pixel on the raster layer fed as input

³ Clip-raster-by-mask-layer tool allows the extraction of selected feature of a raster layer using a mask-layer that contains the shapes of the selected features in vector-layer format.

Table 4.1: Documentation of slopes and azimuths of north, west, south and east facing parts of rooftops in Kalwaria city

Building ID	Average slope (degrees)				Average azimuth (degrees)			
	North face	West face	South face	East face	North face	West face	South face	East face
1	3.197	1.44	0.715	3.603	51.57 3	95.714	216.95 4	338.53 6
2	10.229	2.668	4.742	8.52	28.48 3	115.58 6	228.18 3	333.47 4
3	1.824	0	6.657	9.707	42.55	0	257.91 2	300.36 5

[Source: own study]

Besides the azimuth and slope of the roofs, the yearly in-plane irradiation also depends on the latitude, altitude, weather, shading, etc. PVGIS, a solar irradiation database provided by the European Commission (European Commission, 2017), considered these factors in the solar irradiation model. Using PVGIS, another database was created for this study by extracting the yearly in-plane irradiation in Kalwaria for several combinations of rooftop slopes and azimuths. The slopes considered for the database was 0°-35° with an interval of 5° and the azimuths varied from 0° – 360° with an interval of 15°. The data points collected were processed in MATLAB software to fit the curve in a polynomial equation representing the function in equation 4.1

$$\text{Yearly in – plane irradiation} = f(\text{Slope}, \text{Azimuth}) \quad (4.1)$$

The function obtained was

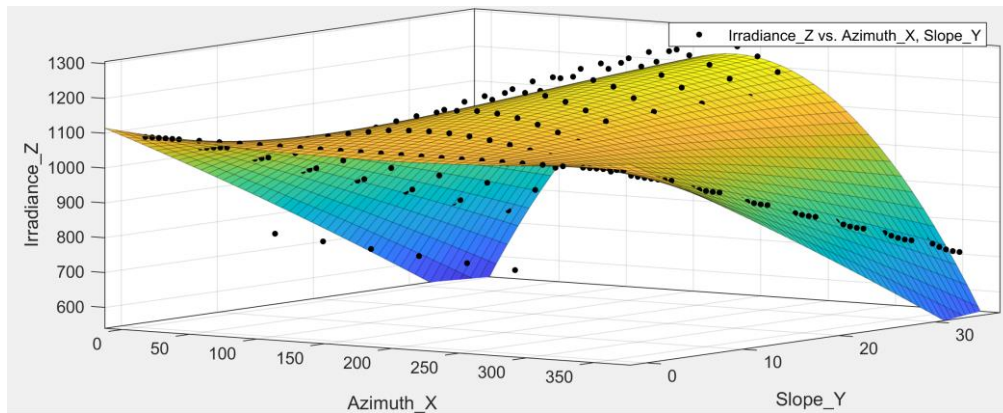
$$f(x, y) = p_{00} + p_{10} \cdot x + p_{01} \cdot y + p_{20} \cdot x^2 + p_{11} \cdot x \cdot y + p_{02} \cdot y^2 + p_{03} \cdot x^3 + p_{21} \cdot x^2 \cdot y + p_{12} \cdot x \cdot y^2 \quad (4.2)$$

[kWh.m²/year]

Where x is the azimuth, y is the slope and p_{ij} values are (with a confidence interval of 95%):

$$\begin{array}{lll}
 p_{00} = 1087 & p_{10} = 1.099 \times 10^{-9} & p_{01} = -12.9 \\
 p_{20} = -6.348 \times 10^{-12} & p_{11} = 0.2091 & p_{02} = -0.04963 \\
 p_{30} = 1.008 \times 10^{-14} & p_{21} = -5.761 \times 10^{-4} & p_{12} = -1.821 \times 10^{-5}
 \end{array}$$

The above model had an R-squared value of 0.9793 and an adjusted R-squared value of 0.9787. Fig 3.2 shows the graphical representation of the model.



[Source: own study]

Figure 4.3: In-plane solar irradiance as a function of roof-slope and roof-azimuth

For each face of the roof (north, south, east and west), the yearly in-plane insolation was calculated using equation 4.2. The total solar energy that can be collected on every rooftop was estimated by adding the solar energy received on each face of the roof. Assuming a solar PV module efficiency of 20%, the maximum solar PV electricity was also calculated. The energy-balance calculations were performed and documented on Microsoft Excel.

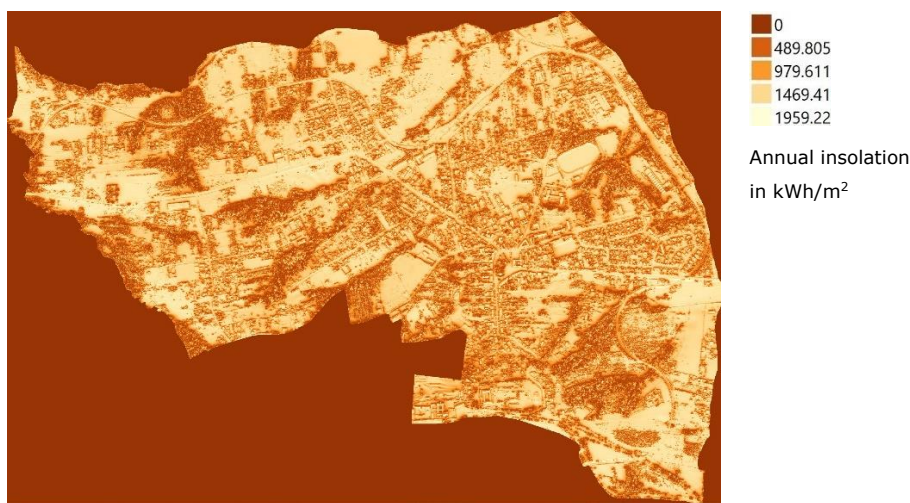
4.1.2 Method 2: estimating solar PV output using solar radiation model of SAGA GIS

To create a solar irradiation map, the DSM of the city was imported into SAGA GIS, to be processed by the *Potential Incoming Solar Radiation* tool of SAGA GIS. The tool also allows the manipulation of other data such as

- Value of the solar constant (W/m^2). This was set to $1367 W/m^2$
- Sky view factor which can either be input as a raster-layer or the option to use local sky view factor can be switched on. In this analysis, the local sky-view factor was used.
- Shadowing options can either be 'slim' if only grid node's shadows are to be traced or 'fat' if the entire cell's shadows shadow is to be traced. For the current project, 'fat' analysis was used.

- Location can be set either manually or by using the data from the DSM.
- The time-period of calculation of insolation can be at a particular hour, on a particular day or for a range of days. The time-step/resolution for a day can be specified in terms of number of hours; if time-period is specified as a range of days, the time-step can also be specified in terms of the number of days. For the present analysis, the time-period chosen was from 1st January to 31st December of the year 2020. The time-step chosen for the period of the entirety of the year 2020 was 5 days; and for each day analysed 1 hour was the resolution.
- Atmospheric effects
- The units can be kWh/m², kJ/m² or J/cm².

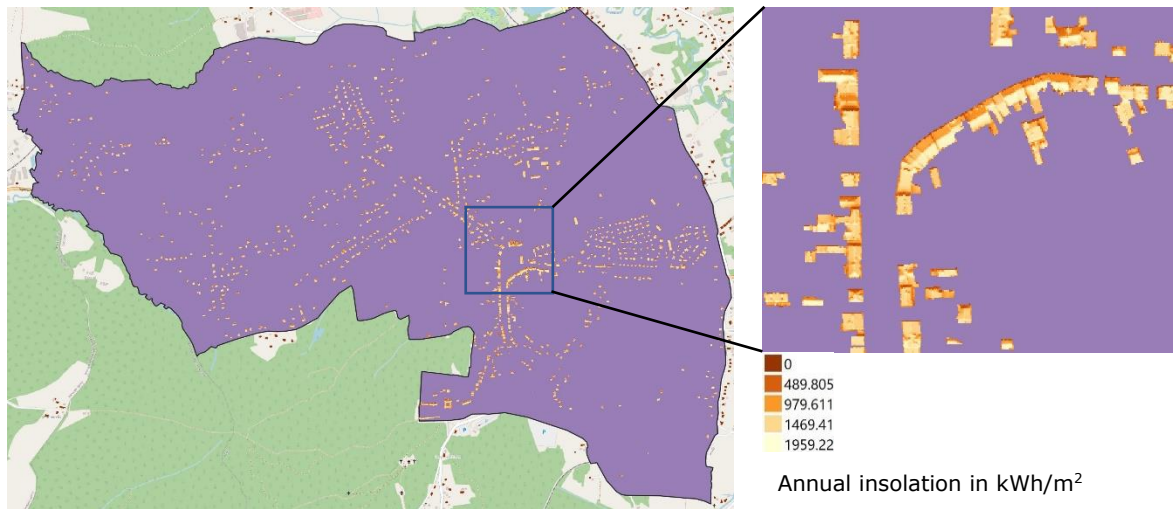
The inputs specified above produced the following solar insolation map (Figure 4.3) in a raster format where each pixel, of size 1 m x 1 m, contains the data of the amount of insolation obtained on that cell over the course of the year 2020.



[Source: own study]

Figure 4.4: Total solar insolation in the year 2020 in kWh/m² units

This raster layer (Figure 4.3) was used to extract the insolation only on the rooftops of the residential buildings identified previously (Figure 4.1). To do so, the solar insolation layer was imported into QGIS from SAGA GIS. Using the *clip raster by mask layer* tool of QGIS, insolation received only on the rooftops were extracted as shown in Figure 4.4.

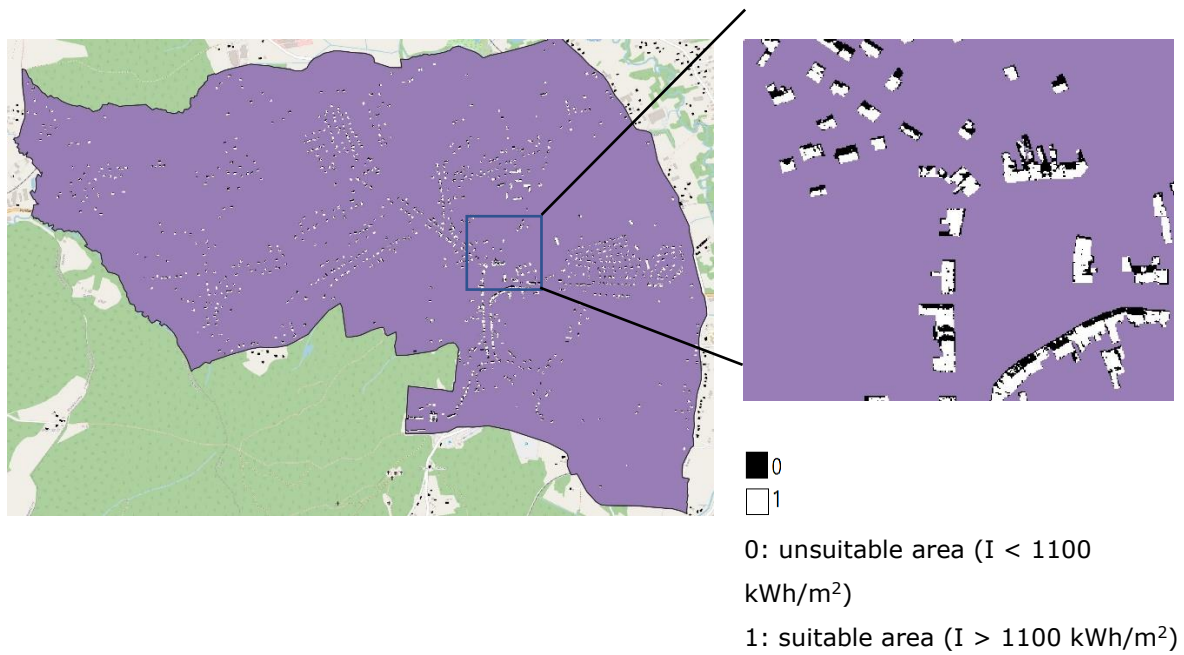


[Source: own study]

Figure 4.5: Annual rooftop insolation in Kalwaria city for the year 2020 (kWh/m²)

The next step was to estimate the maximum rooftop solar PV capacity that can be installed in Kalwaria city. However, it is not economical to install solar panels everywhere on the roof. Therefore, regions that receive above 1100 kWh/m² (Kereush and Perovych, 2017) were to be selected. Using the 'raster calculator' tool, pixels of the insolation layer with values greater than equal to 1100 kWh/m² were assigned a value of 1 and the other were assigned values of 0 (a binary raster layer). The resulting layer is shown in Figure 4.5.

The 'raster calculator' tool also allows the multiplication of the data contained in the pixels of a raster layer with the data contained in the same pixels in another raster layer. The raster layers represented by Figures 4.5 and 4.4 were multiplied to get an output raster where solar-unsuitable pixels will have a value of 0 and the solar-suitable pixels will have a value equal to their annual insolation. The resulting raster layer shown in Figure 4.6.



[Source: own study]

Figure 4.6: Solar suitable rooftop areas where annual insolation is greater than or equal to 1100 kWh/m²

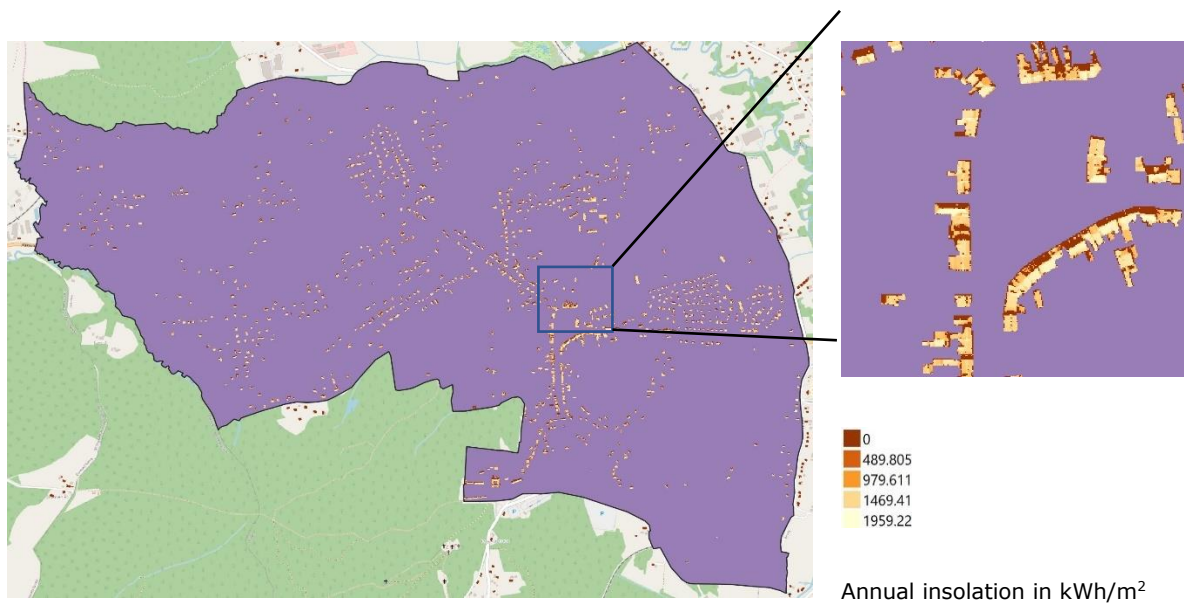


Figure 4.7: Insolation on solar suitable rooftop areas (kWh/m²)

The raster layer in Figure 4.6 obtained from the solar irradiation model in SAGA GIS can account for the shadows due to vegetation, neighbouring buildings, chimneys and dormers. However, the dormers and chimneys themselves had not been excluded yet. Therefore, to calculate the usable solar insolation on the roof tops, it was assumed that only 90% of the area identified

previously as solar suitable areas could be used for generating solar PV power. With these assumptions, it was possible calculate the usable annual insolation on the rooftops.

To determine the maximum rooftop solar PV capacity, the maximum number of solar PV modules that can be installed on the rooftops have to be estimated. The model of the solar PV module selected for this estimation is NU-JC370 supplied by Sharp Corporation:

Table 4.2: Properties of the solar PV module used as a standard for rooftop solar PV power estimation

Module properties (at NMOT)	Value
Module model	NU-JC370
Maximum power (Watt)	370
Length (mm)	1765
Width (mm)	1048

[source: <https://kotly.com/pl/1643-modul-fotowoltaiczny-sharp-nu-jc370-mono-370w-bez-transportu.html>]

The number of NU-JC370 solar PV modules that can be fitted on each roof was estimated by rounding-down the quotient obtained dividing the usable rooftop area (excluding chimneys, dormers, edges and shadowed areas) by the area of each module to the nearest whole-number. The product of this module-count with the peak power of NU-JC370 gave the rooftop solar PV capacity for Kalwaria city.

The maximum amount of solar PV energy that could have been obtained using the installed capacity was estimated using equation 2.8. For this calculation it was assumed that the modules have a performance ratio of 75%. The performance ratio was obtained by assuming losses due to inverters, temperature of module, DC cables, AC cables, weak irradiation, dust, snow, shadowing, etc.

4.2 City-level energy planning using urban heat demand model

In Wyrwa, 2019, an energy-economic model that was built to identify the thermo-modernisation of buildings and upgrade in their heating technologies required to meet the energy demands and emission constraints in cities where the main causes of emission are the emissions from devices used for space

heating. The model utilized geo-referenced datasets of buildings which enabled the processing of the data of each building. This model was adapted for the aims of this project.

The model was designed to solve a mixed-integer programming (MIP) problem where a verdict can be made for each household in Kalwaria Zebrzydowska. The verdict pertains to deciding how many of the following changes should be adopted by each of the 1090 single family houses in the city

- Replacement of windows
- Thermo-modernisation of outer walls
- Insulation of roofs
- Replacement or modernisation of the central heating system
- Installation of rooftop solar PV modules

The inputs for the model include, for each building, the existing thermal state (type of windows, roofs and wall insulation), year of construction, heating demand, area of the perimeter, number of floors, heating devices used and their characteristics such as efficiency and data of the cost of each retrofit measure.

The heating demand for each building was obtained from the TABULA project (IEE Project TABULA, 2012). The project contains data of Polish national building typology which were categorized into many stocks with respect to their construction period and their functions, such as one-family and multi-family. Due to smaller values of heat transfer-coefficients of the materials used for the building's construction, newer buildings have lower heat demands. On the contrary, older buildings have higher heat demands in comparison. The heat demand also depends on the thermal retrofitting that the building had undergone.

Very often boilers, used for burning hard coal which is the fuel used by 90% of the buildings in Kalwaria Zebrzydowska (Wyrwa, 2019), is oversized. The model can either decide to let the heating technology remain the same or decide to adopt a heating technology with a capacity that is better suited for the energy demand of the building. The model compares three categories of capacities: (i) $c \leq 14$ kW (ii) $14 \text{ kW} \leq c \leq 19$ kW (iii) $19 \text{ kW} \leq c \leq 25$. The heating technologies considered for this project have been listed in Table 4.3 along with their

efficiencies of power production, efficiency of transmission, regulation and accumulation, thermal capacity, investment costs and fuel prices.

Table 4.3: Techno-economic parameters of heating technologies

Technology type	Fuel	Efficiency [%]	Efficiency of transmission, regulation and accumulation process [%]	Thermal capacity, c [kW]	Investment costs [PLN/kW]	Fuel price [PLN/kWh]
HC_1_14	Hard coal	70	84	$c \leq 14$	0	0.13
HC_1_19	Hard coal	70	84	$14 \leq c \leq 19$	0	0.13
HC_1_25	Hard coal	70	84	$c > 19$	0	0.13
GAS_1_19	Natural gas	90	84	$c > 19$	0	0.25
HC_5_14	Hard coal	91	84	$c \leq 14$	744	0.16
HC_5_19	Hard coal	91	84	$14 \leq c \leq 19$	569	0.16
HC_5_25	Hard coal	91	84	$c > 19$	465	0.16
GAS_14	Natural gas	95	84	$c \leq 14$	300	0.25
GAS_19	Natural gas	95	84	$14 \leq c \leq 19$	270	0.25
GAS_25	Natural gas	95	84	$c > 19$	250	0.25
EE_14	Electricity	99	90	$c \leq 14$	331	0.38
EE_19	Electricity	99	90	$14 \leq c \leq 19$	382	0.38
EE_25	Electricity	99	90	$c > 19$	508	0.38
OO_14	Fuel oil	95	84	$c \leq 14$	506	0.43
OO_19	Fuel oil	95	84	$14 \leq c \leq 19$	423	0.43
OO_25	Fuel oil	95	84	$c > 19$	366	0.43

[source: Wyrwa, 2019]

The model can also choose to thermo-modernize the building. Replacement of windows rests on the assumption that, if chosen to do so, the old windows will be replaced by a new double-glazed window with dimensions of 1160 x 1400 mm whose overall replacement cost will be 950 PLN. Furthermore, the ratio of window-area to floor-area for each floor, where people will live, should be 1:8; however, since not every part of a floor will be inhabited 2 windows will be subtracted from the number obtained from the math based on the "1:8" ratio (Wyrwa, 2019).

With respect to wall insulation, it was presumed that polystyrene foam will be the insulating material in the walls. The surface area of the building whose walls will be insulated was estimated by assuming that each building assumes

the shape of a square prism and each floor has a height of 3.5 meter. The cost of wall refurbishment, including labour was estimated at 80 PLN per square meter. Finally, to thermo-modernize the roofs it was presumed that mineral wool will be used; this will yield an estimate of 100 PLN per square meter of roof. The roof area was assumed equal to the area of the perimeter of the building, which was calculated using GIS tools for each building.

With respect to rooftop solar PV installations, a choice can be made, by the model, for every building on whether it is economically reasonable to install PV modules on its roof. The total cost of the installation was obtained by estimating the CAPEX and OPEX of the PV module over the course of 15 years (the lifespan assumed for all technologies in this project). It was also assumed that the electricity generated will be stored in the grid so that it can be reclaimed for future use. The calculation of the CAPEX, OPEX and the money saved (from using the stored solar energy) was subject to and discounting and inflation rates.

The model, which functions as a bottom-up approach to inspecting buildings, was built in the software called GAMS. It was also coupled with QGIS so that building-data can be supplied in a geo-referenced manner; furthermore, it also enables the processing and visualisation of results on QGIS. The following equations and math were used to algebraically represent the problem statement in GAMS:

4.2.1 Defining global sets

The following global sets were used for writing the algorithm for the model:

$id \in \{1, 2, 3, \dots, 1090\}$	-building ID/number
$o \in \{\text{good}, \text{bad}\}$	-windows (good-efficient, bad-inefficient)
$s \in \{\text{good}, \text{bad}\}$	-wall insulation (good-efficient, bad-inefficient)
$d \in \{\text{good}, \text{bad}\}$	-roof insulation (good-efficient, bad-inefficient)
$t \in \{\text{HC}_1_{14}, \text{HC}_1_{19}, \text{HC}_1_{25}, \text{GAS}_1_{19}, \text{HC}_5_{14}, \text{HC}_5_{19}, \text{HC}_5_{25}, \text{GAS}_{14}, \text{GAS}_{19}, \text{GAS}_{25}\}$	-heating technology

EE_14, EE_19, EE_25, OO_14,
OO_19, OO_25}

$p \in \{PM10, SO2, BaP, CO2\}$

-pollutant

$rp \in \{A, B, C, D, E, F, G\}$

-classes based on year of construction

$RES \in \{Solar, No_Solar\}$

-Renewable energy generation
(Solar—renewable energy produced
with solar PV modules, No_Solar—
renewable energy is not produced)

4.2.2 Building representation

Each building is defined by a set (with the elements mentioned above) like so:

$\{id, o, s, d, t, rp, RES\}$

Each element depicting a property/state of the building. 'id' represents the identification number assigned to the building, 'o' represent the state of the windows, 's' represents the state of the walls, 'd' represents the state of the roofs, 't' represents the type of heating-technology, 'rp' represents the time-period of construction of the building and 'RES' represents whether the building has rooftop solar PV modules installed or not.

4.2.3 Decision variable

The decision variable φ is a binary variable. And for each possible building configuration, a decision is made whether that configuration is the best choice for that building. i.e.,

$$\varphi_{(id,o,s,t,rp,RES)} = \begin{cases} 0, & \text{if the configuration is not chosen} \\ 1, & \text{if the configuration is chosen} \end{cases} \quad (4.3)$$

The decision is made in a way that the total cost is minimum.

4.2.4 Equations

For a building with id 'I' there are 1792 possible configurations that it can accept, including the one it had in the beginning. However, only one configuration can be selected. Hence,

$$\sum_o \sum_s \sum_d \sum_t \sum_{rp} \sum_{RES} \Phi_{(id,o,s,t,rp,RES)} = 1 \quad (4.4)$$

The function to optimize is the cost of the changes/ additions implemented in the energy system, c :

$$C_T = \sum_{id} \sum_o \sum_s \sum_d \sum_t \sum_{rp} \sum_{RES} C_{(id,o,s,t,rp,RES)} \cdot \Phi_{(id,o,s,t,rp,RES)} \quad (4.5)$$

Where, C_T is the total cost and

$$C = F + I^o + I^s + I^d + I^t + I^{rp} + I^{RES} - R \quad (4.6)$$

Where, F is the cost of the fuel used by the heating device for its life time (for consistency and ease of calculation, the life time of all devices including solar PV modules have been considered to be 15 years, even though gas boilers and solar panels can last more than 20 years), I^x is the investment cost of the modification or instalment of feature 'x', R is the revenue obtained from selling the electricity generated from the rooftop solar PV modules.

To calculate the emissions of air pollutants, the final fuel consumption was required which, in turn, depended on the heated area. The total heated area of a building with identification number 'id', A^f , was calculated using the perimeter-area of the buildings using GIS tools like so:

$$A^f_{id} = A^z_{id} \cdot l \cdot cor^f_{id} \quad (4.7)$$

A^z_{id} was the area of the outer counter of the building [m²], l is the number of floors in the building and cor^f_{id} is the heated area calibration ratio of building 'id' and is assumed to be 0.8 for all buildings for ease of calculation. In reality, cor^f differs from single-family buildings and multi-family buildings (Wyrwa and Chen, 2017).

Furthermore, the final energy consumption is calculated from the useful energy demand in homes by factoring the efficiency of energy transmission, regulation and accumulation, η .

$$E_{id} = \frac{A_{id}^f \cdot Q_{id}^u}{\eta} \quad (4.8)$$

Where, E_{id} is the final energy consumption in kWh/year, Q_{id}^u is the specific heat demand for the building. Q_{id}^u can be one of 56 possible values that depends on the building configuration (o-2 possible values, s-2 possible values, d-2 possible values and rp-7 possible values; totalling 56 combinations).

Finally the emissions were estimated using the emission factors presented in Table 4.4 (Wyrwa and Chen, 2017).

Table 4.4: Emission factors of various heating technologies

Technology	Particulate matter -PM10 [g/GJ]	Carbon dioxide -CO2 [kg/GJ]	Benzo(a)Pyrene -BaP [mg/GJ]	Sulfur dioxide -SO2 [g/GJ]
Hard coal 1	225	93.74	150	900
Hard coal 5	78	93.74	55	450
Natural gas	0.5	55.82	0	0.5
Fuel oil	2	76.59	0.08	70
Electricity	0	0	0	0

[source: Wyrwa and Chen, 2017]

4.3 Financial assessment of rooftop solar PV instalments

Before the model could decide to whether rooftop solar PV instalments will be accepted or refused, the model should have information about the total cost of having PV modules on the roof for 15 years and the revenue that can be yielded from it for each building. Therefore, the net present value (NPV) of the potential PV installation on each roof was estimated and fed as input to the model.

The CAPEX for each building is the sum of the cost of all NU-JC370 PV module installed, cost of inverters, and the cost of installing the module (labour and wiring). All these factors were assumed to be included in the CAPEX cost of 4500 PLN/kWp.

OPEX was comprised of the maintenance fee. Fee for replacement of parts was avoided since it was assumed that the quality of the installations were

excellent. For installations up to 1.5 kWp, the annual OPEX was considered to be 10% of CAPEX. And for installations greater than 1.5 kWp, OPEX was considered to be 4% of CAPEX.

In Poland, the grid provides the facility to act as a storage facility for the renewable energy that is generated and sent into the grid. When extracted back, 85% of the sent power is available to the solar PV owner. For example, if the household generates 10 MWh of electricity in the summer and sends it to the grid, the household can store the energy in the grid and reclaim a maximum of 8.5 MWh of energy from the grid in winter, free of charge. This is due to the transmission losses of electricity.

For the base year, the price of electricity as sold to the households is 0.6-0.8 PLN/kWh. Since this is the cost that will be avoided while reclaiming the stored electricity, it can be assumed that the financial gain of the process is equivalent to selling the obtained renewable energy to the grid for the same cost as the retail-price of electricity, however, with a loss of 15% in the revenue. Nevertheless, to understand the effect of the revenue rate on the thermo-modernisation, heating technology and amount of solar PV installation, a sensitivity analysis was performed by varying the revenue rate from 0.2-1 PLN/kWh. Since only 85% of the energy can be reclaimed, it is assumed that the households' revenue will be cut short by 15% of what it would be without the transmission losses.

The discount rate was assumed to be 5% and a flat inflation rate of 2% was also assumed to calculate the NPV of each building, 'ID', using the following the formula:

$$NPV_{ID} = \left(\sum_{i=0}^{15} \left(Revenue_{i,ID} \cdot \left[\frac{1}{(1+D)} \right]^i - OPEX_{i,ID} \cdot \left[\frac{IR}{(1+D)} \right]^i \right) \right) - CAPEX_{ID} \quad (4.9)$$

Where, IR is the inflation rate and D is the discounting rate. A part of the calculations have been presented in Appendix I to show how the math was performed.

5 Results

5.1 Rooftop solar PV output

The two methods used to estimate the potential rooftop solar PV energy that can be generated from 1090 houses in Kalwaria city mainly differ in the method used to estimate the annual solar insolation. The results from both methods have been tabulated below in Table 5.1.

Table 5.1: Comparison of results from the solar irradiation models of derived from PVGIS and SAGA GIS

Energy indicators	Method 1	Method 2
Total annual insolation (GWh)	146.29	174.07
Maximum power generated from Kalwaria city (MWp)	-	16.16
Maximum PV electricity that can be generated annually(GWh)	8.77	18.64

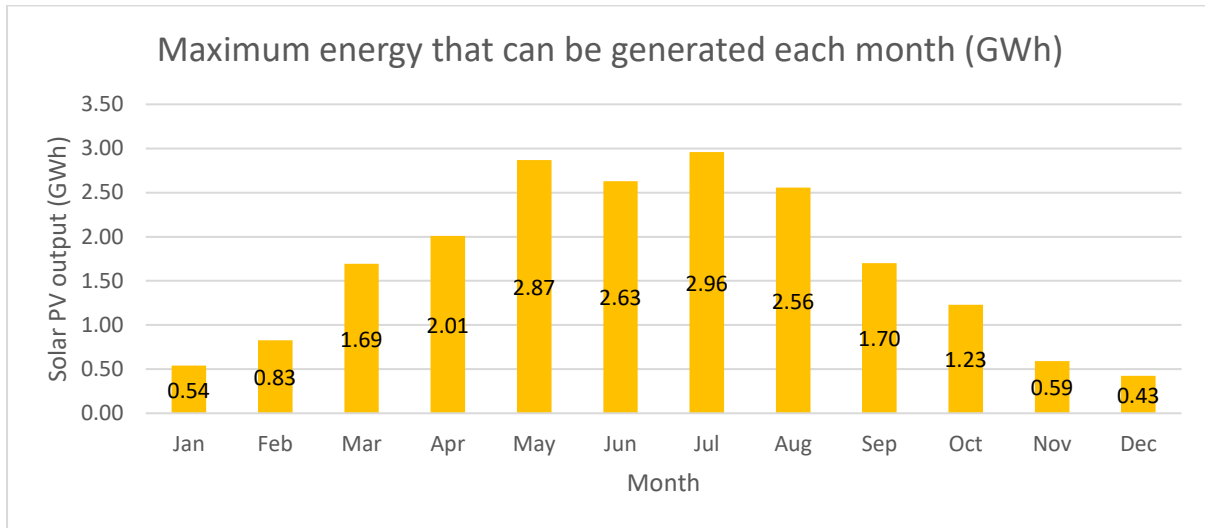
[source: own study]

The total annual insolation estimated by method 2 is 18.9 % larger than that estimated by method 1. However, the maximum solar PV energy that can be generated as estimated by method 2 is 112.5 % larger than that estimated by method 1. However, owing to the higher precision of method 2 its results can be deemed to be more accurate.

An advantage of method 2 is that it allows the calculation of the maximum capacity of the rooftop solar PV installations feasible which is not possible using method 1. It showed that a maximum of 16.16 MWp can be installed in Kalwaria city which is expected to produce 18.64 GWh of energy. The average capacity factor for PV systems in Poland is 10.9 % according to Jurasz, Dąbek and Campana, 2020, which implies 15.43 GWh of photovoltaic energy can be produced using the capacity estimated from method 2; this value is comparable to the PV energy output estimated by method 2 as well.

Method 2 was repeated using the insolation data of each month in the year 2020. It was assumed that the area suitable for placing the solar panels was the same as that obtained previously for the annual solar PV output. The result was a monthly solar PV output profile as shown in Figure 5.1. As

expected, the largest amount of electricity is obtained during the summer and early autumn.

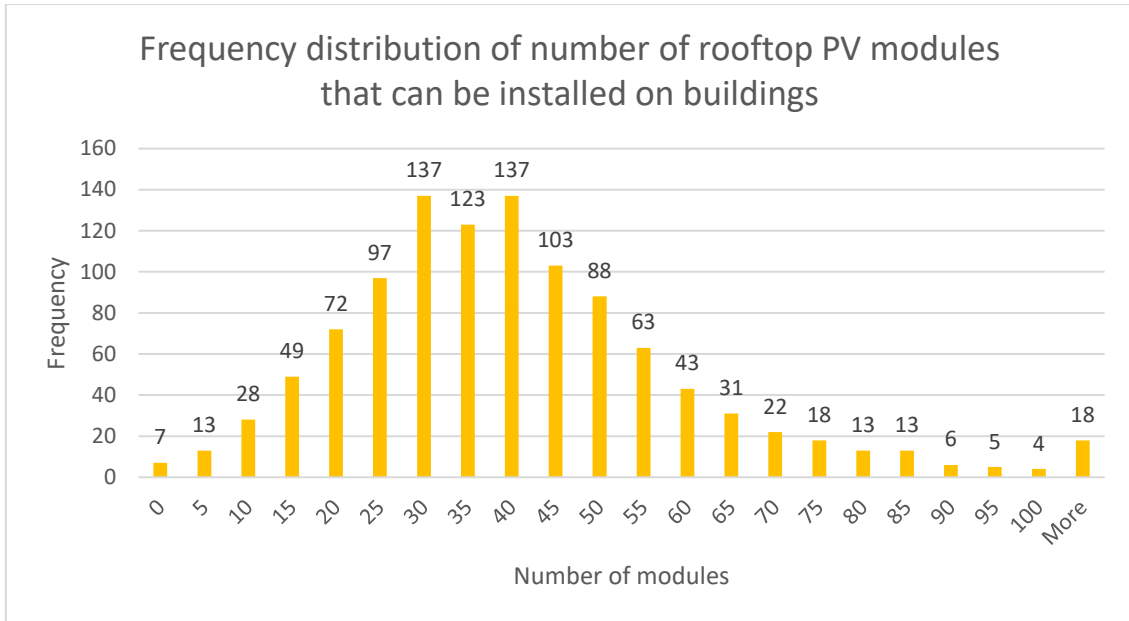


[source: own study]

Figure 5.1: Monthly rooftop solar PV output profile in Kalwaria

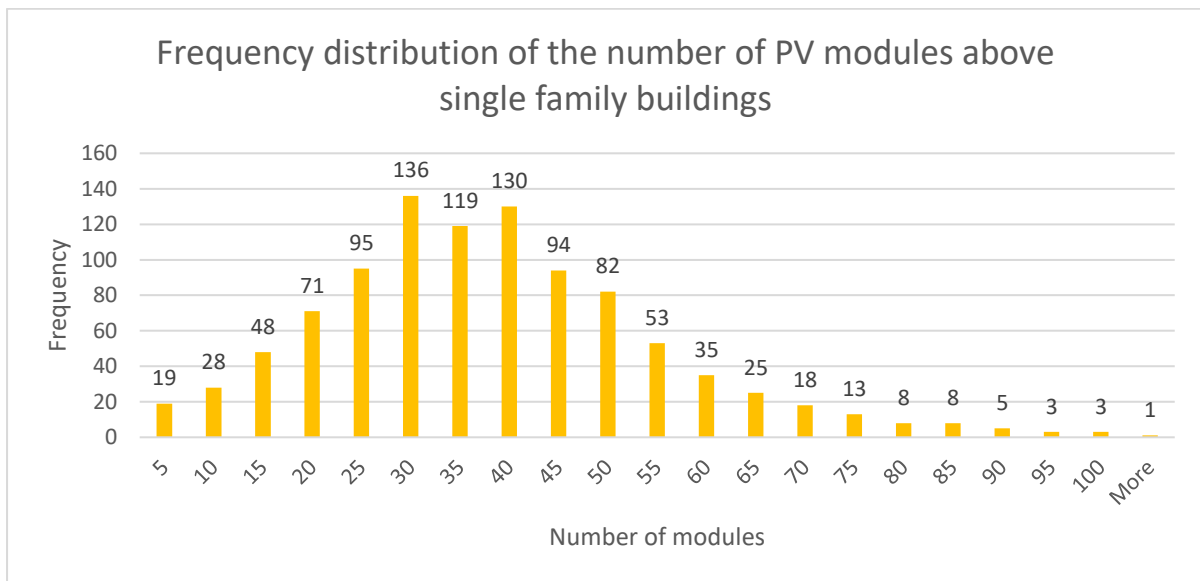
Figure 5.2 shows the frequency distribution of the number of solar modules that can be installed on rooftops of house in Kalwaria city. Each data point on the x-axis can be interpreted as the upper limit of the interval between the current and previous x-axis value. For example, at x-axis value of 5, the frequency is 13; this implies that there are 13 buildings where the number of PV modules is greater than zero but less than 5. It can be seen that most houses can have between 15-60 solar modules on the roofs. There are even some buildings with the ability sustain more than 100 PV modules.

An average single-family household in Poland requires 5-6 kWp of power which is equivalent to 14 PV modules. As it can be seen from Figure 5.3 almost 91% of the single-family households have roofs suitable for installing more than 15 PV modules.



[source: own study]

Figure 5.2: Frequency distribution of the number of solar PV modules that can be installed on each rooftop



[source: own study]

Figure 5.3: Frequency distribution of the number of rooftop PV modules on single family houses

5.2 Energy system modelling—deciding retrofitting measures

The energy-economic model created for Kalwaria Zebrzydowska allowed the flexibility of choosing the types of retrofit measures the user would like to examine/include in the study. Therefore, using the energy-economic model the

effect of different retrofit measure could be examined individually. This allowed for a sensitivity analyses of the effect of thermo-modernisation and heating technology on emissions and total costs. Two broad cases were analysed: with rooftop solar PV installations and without. The purpose of this discrimination was to test if the money saved by selling the solar energy could propel further investments in energy efficient measures and emission reduction.

5.2.1 Without rooftop solar PV

The following scenarios were examined for the case without solar PV installations.

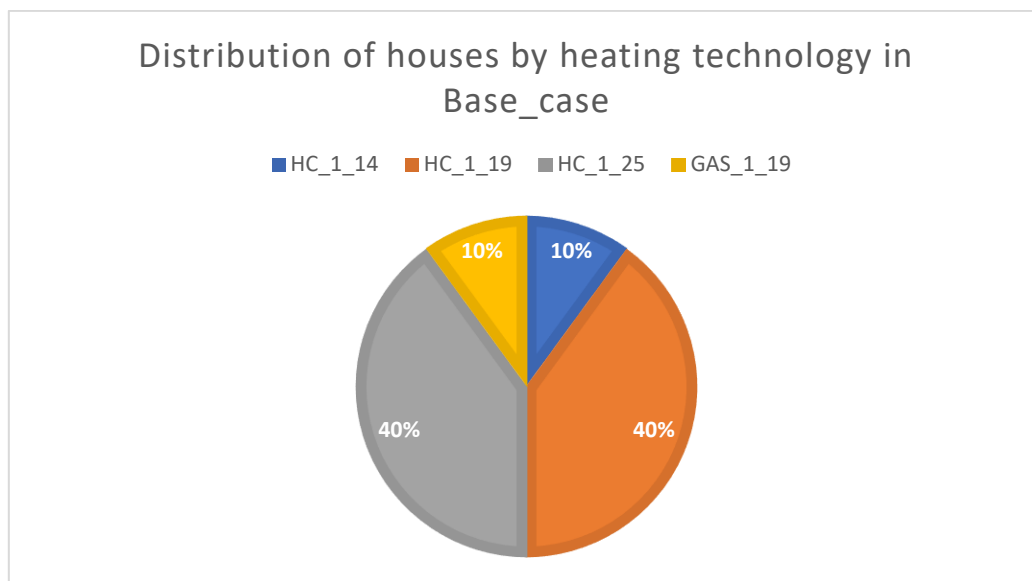
Table 5.2: Description of cases analysed in the model

Name	Description
Base_Case	Original scenario; no thermo-modernisation and no upgrade of heating-technologies
HeatTech_EE	Only electric heating will be applied to all buildings while still implementing thermo-modernisation.
HeatTech_HC5	Only hard coal boilers of type HC_5 will be applied to all buildings while still implementing thermo-modernisation.
HeatTech_GAS	Only natural gas-based boilers will be applied to all buildings while still implementing thermo-modernisation.
HeatTech_OO	Only fuel oil-based boilers will be applied to all buildings while still implementing thermo-modernisation.
Optimum_Case	The optimum heating technology and thermo-modernisation will be decided by the model
Only_Thermod	Only thermo-modernisation will be applied to the building and not upgrades of the heating technologies

[source: own study]

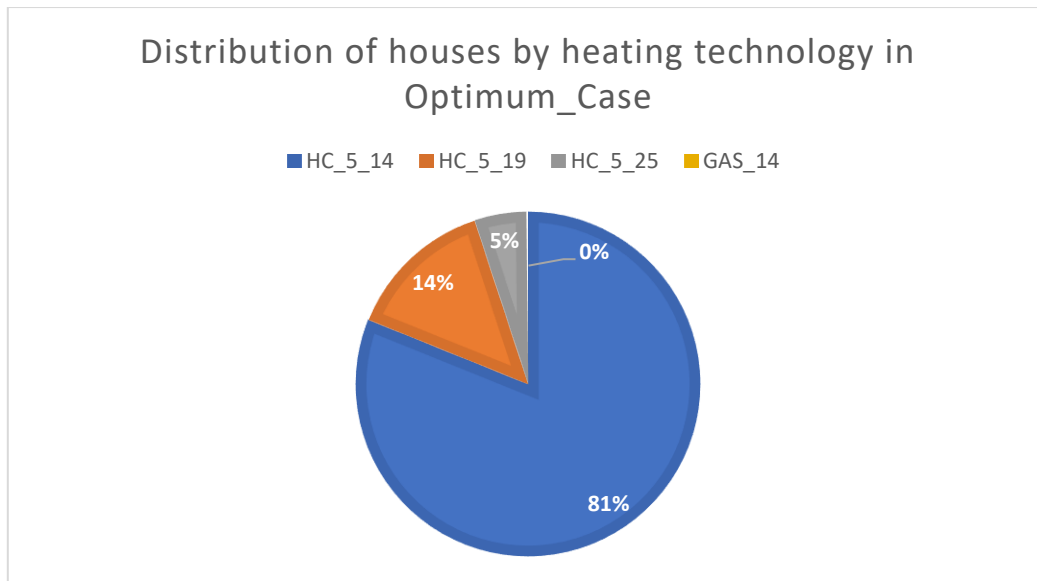
All the above cases did not have any constraints. The only imposition, made using the algorithm of the model, was that the cost of the system (which was the objective function) should be minimum.

Figure 5.4 shows the distribution of houses on the basis of the heating technology they use in the Base_Case. It shows that most houses use hard coal boilers of type one (lower efficiency) with capacity of 25 kW or natural gas boiler of lower efficiency and capacity of 19 kW. Both these technologies account for 80% of the heating demands in Kalwaria Zebrzydowska. Comparing this to the optimum result obtained from the model (shown in Figure 5.5), 81% of the energy demands can be met by hard coal boilers of higher efficiency with a capacity of 14 kW. This proves that most residential buildings in the city had oversized boilers.



[source: own study]

Figure 5.4: Distribution of the type of heating technology used in Base_Case



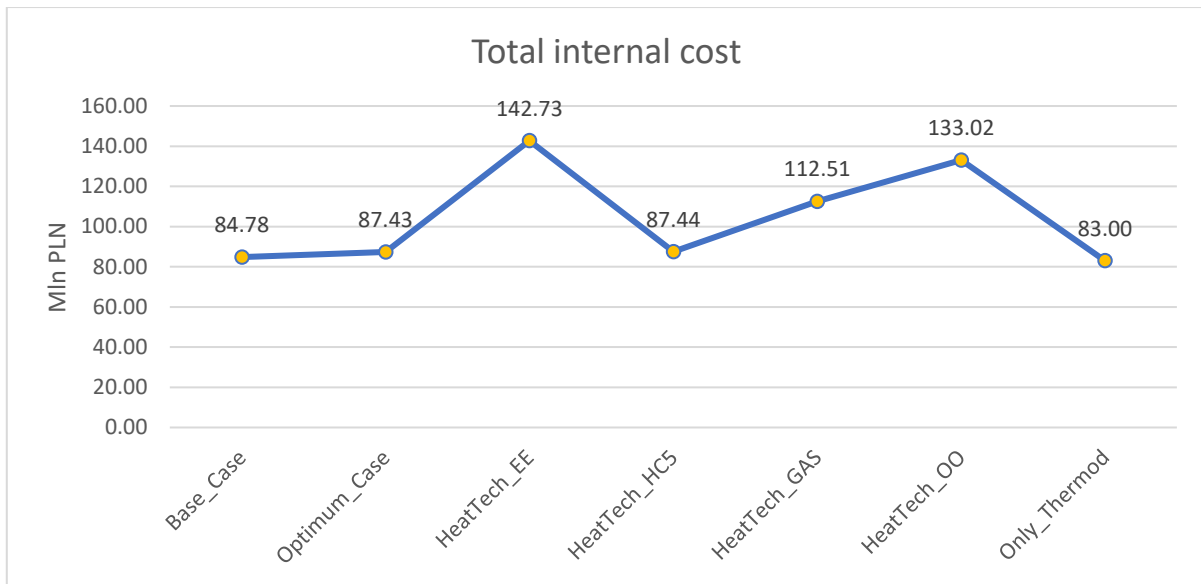
[source: own study]

Figure 5.5: Distribution of the type of heating used in Optimum_Case

Figure 5.6 compares the total internal cost borne by each scenario mentioned in Table 5.2. The total internal cost include cost of all window replacement and wall and roof modification, investment cost of replacing heating technologies and the total cost fuel that will be used for heating for the 15-year lifetime of the heating device. External costs borne out of air pollution has not been included.

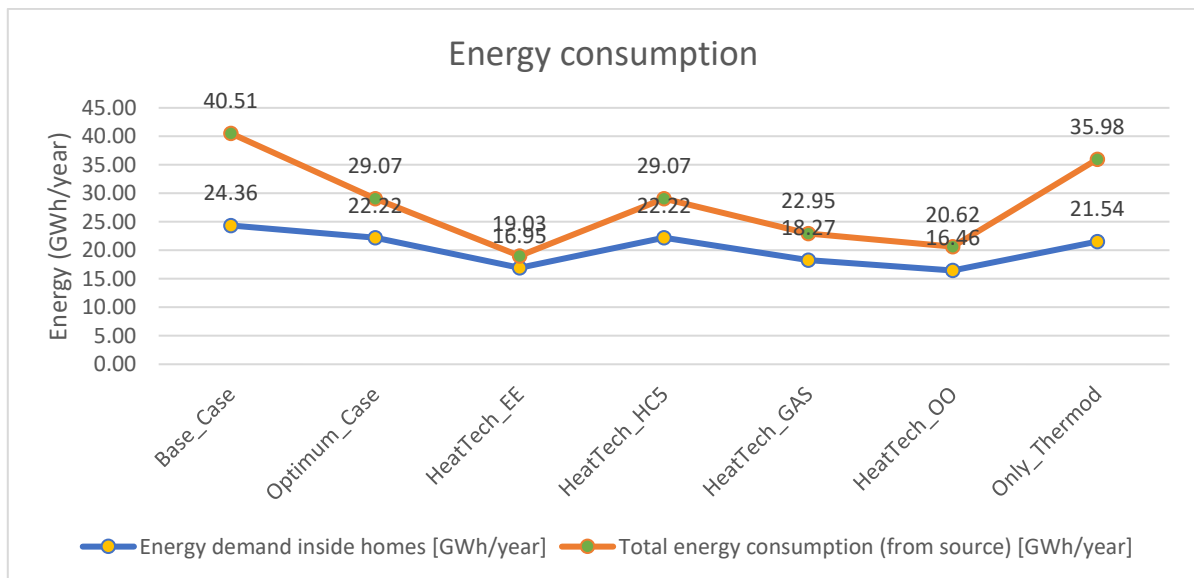
Figure 5.6 shows that compared to the costs incurred for the Base_Case and the Optimum_Case is comparable (84.78 and 87.43 million PLN respectively) despite the major retrofitting applied to the buildings. This is due to the large amount of fuel consumed by the Base_Case owing to the low efficiency of the hard coal boilers (HC_1_14, HC_1_19 and HC_1_25). The difference in the fuel consumed can be observed in Figure 5.7. The Base_Case scenario will consume 40.51 GWh annually whereas the Optimum_Case scenario will only consume 29.07 GWh annually.

Due to the high efficiency of electric heating, fuel oil boilers and gas boilers, the final energy consumed is the lowest among all the scenarios; however, they are also the most expensive which proves the trade-off between energy efficiency and investments.



[source: own study]

Figure 5.6: Total internal cost estimated for each scenario without rooftop PV installations

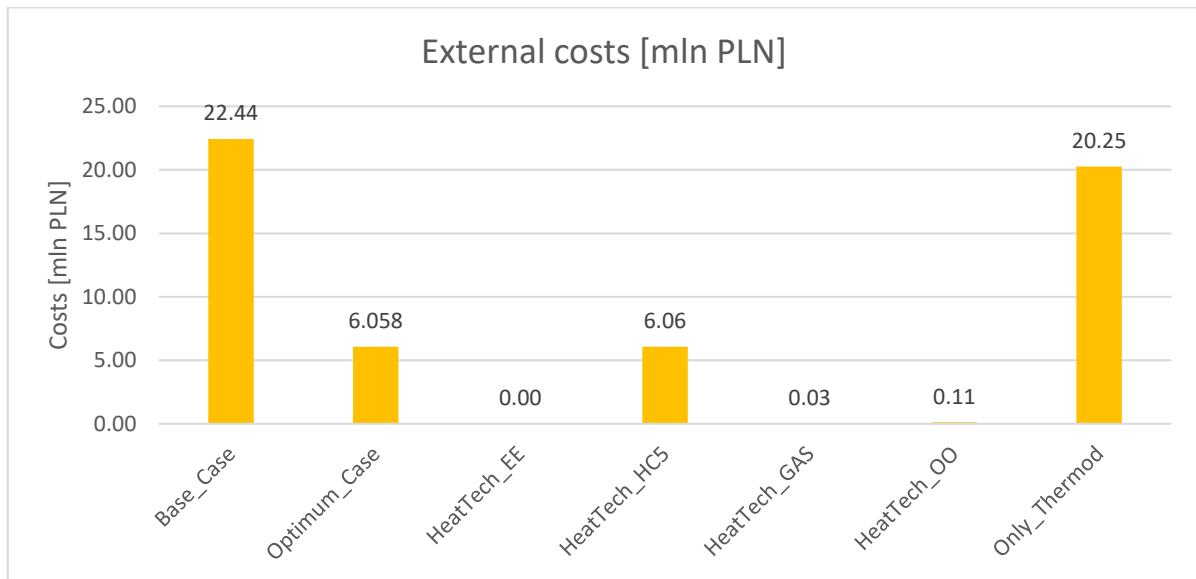


[source: own study]

Figure 5.7: Comparison of energy consumption in each scenario

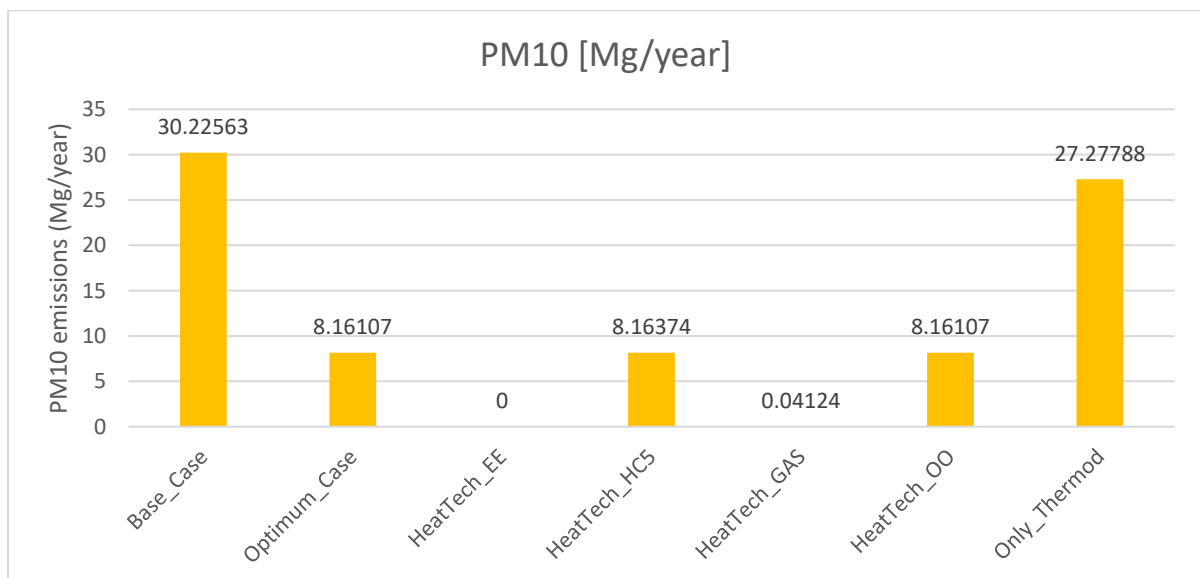
The effect that only thermo-modernisation will have was also examined. Figure 5.6 shows that the Only_Thermod scenario has the least cost of all the scenarios examined. The thermo-modernisation brought down the final fuel consumption from 40.51 to 35.98 GWh/year, a 11.18% reduction, and the heating demands in the house was reduced from 24.36 to 21.54 GWh/year, a 11.57% reduction; However, the absence of any upgrade in heating technology

resulted in higher fuel consumption and thereby increasing the external costs as shown in Figure 5.8.



[source: own study]

Figure 5.8: External costs borne due to PM10 emissions from fuel combustion



[source: own study]

Figure 5.9: Annual PM10 emissions for each scenario

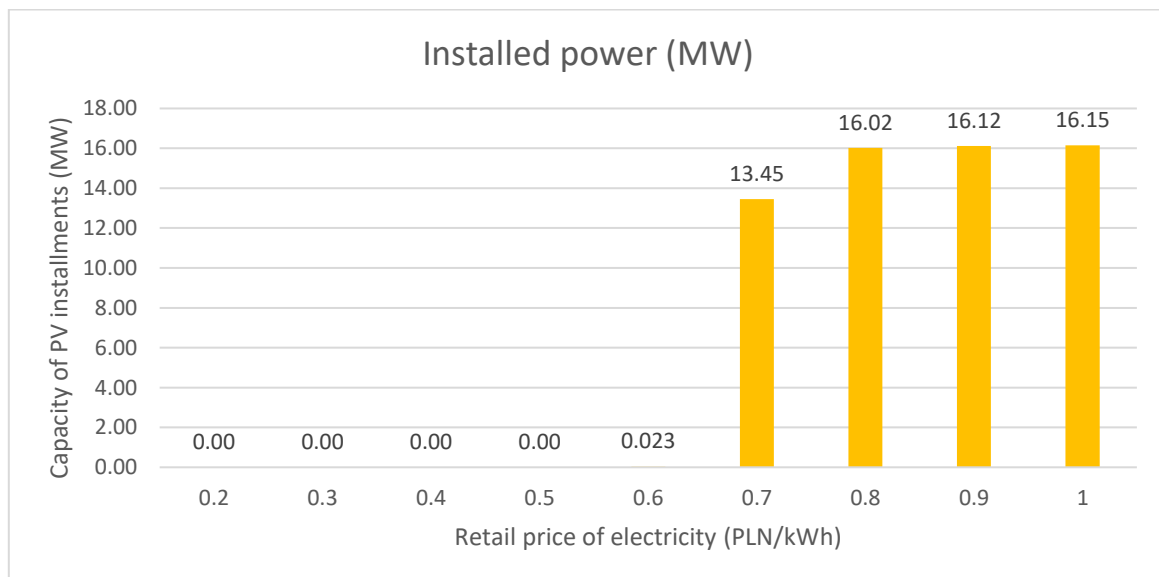
The external costs were calculated at the rate of 49.49 PLN/kg of PM10 emissions. The annual PM10 emissions for each scenario have been shown in Figure 5.9 and it shows that the emissions of Only_Thermod scenario is 2.34 times that of Optimum_Case scenario. Thus, Only_Thermod scenario will have a

total external cost of 20.25 million PLN and the Optimum_Case scenario will have a total external cost of 6.06 million PLN. Thus, the total social cost of Only_Thermod scenario will be higher than the Optimum_Case scenario.

5.2.2 With rooftop solar PV

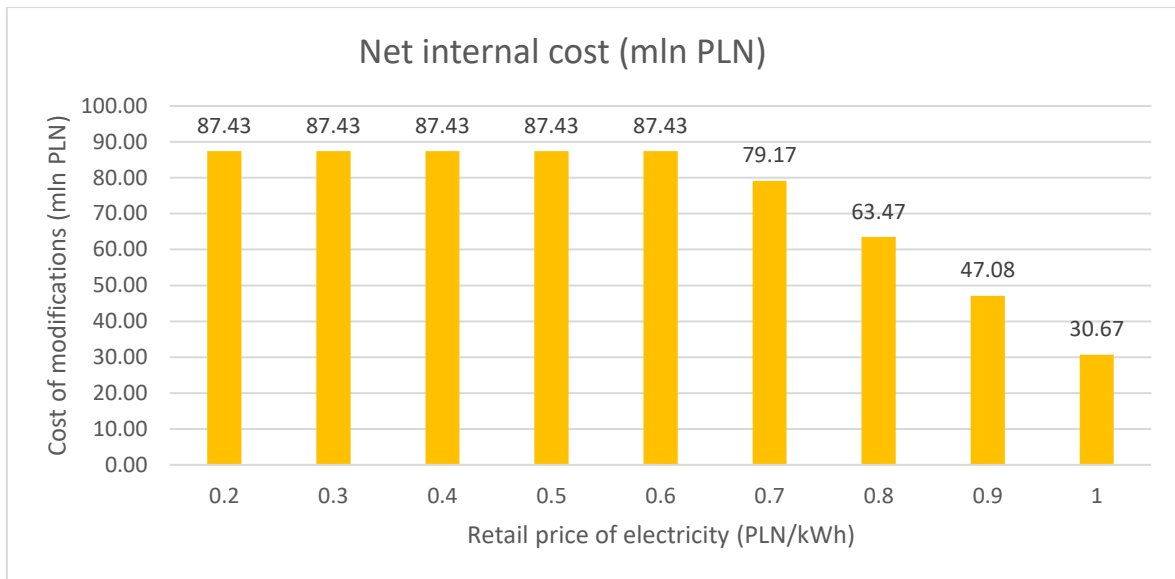
To test the impact of having rooftop solar PV modules, the option to have or not have PV modules installed was enabled in the Optimum_Case. The price for the electricity sold by the households was varied between 0.2 and 1 PLN/kWh.

The variation in the total capacity of solar PV installations can be seen in Figure 5.10. It can be seen that until the cost of electricity reaches between 0.6-0.7 PLN/kWh, it is not financially ideal to install PV modules in the Kalwaria. The reason for this is explained in Figure 5.11 where it can be seen that until the price reaches 0.6-0.7 PLN/kWh, the total internal cost does not reduce below the costs estimated in the Optimum_Case. However, from 0.6-0.7 PLN/kWh, the revenue from the installed PV modules (for 15 years) would surpass the installation costs.



[source: own study]

Figure 5.10: Variation in installed capacity of PV modules with respect to the retail price of electricity



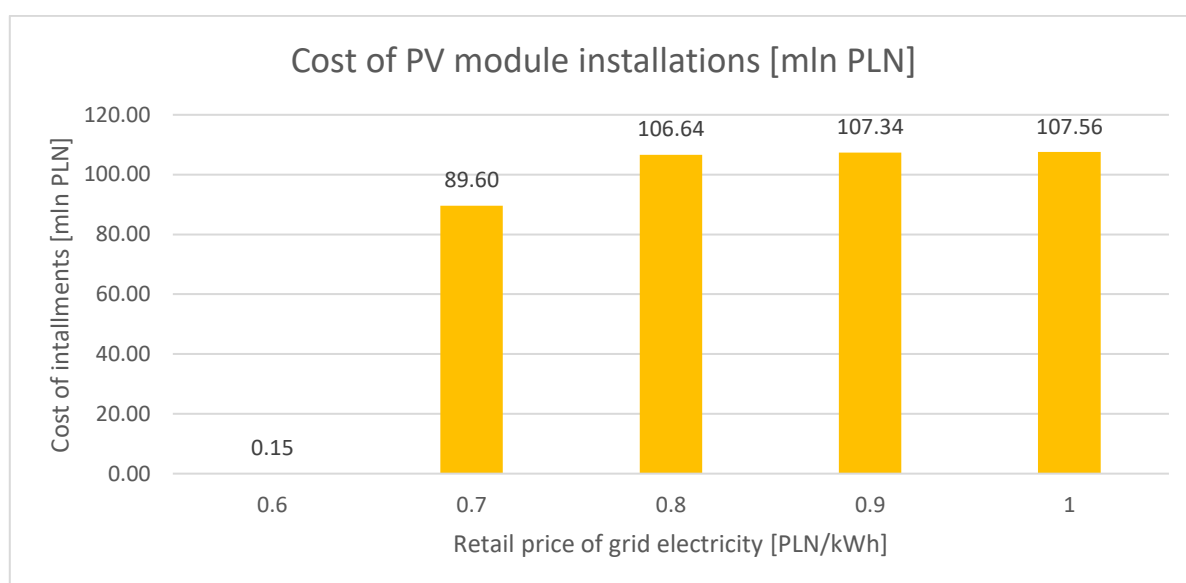
[source: own study]

Figure 5.11: Variation in the total internal cost (of thermo-modernisation, heating technology solar PV installations, fuel costs minus the revenue from PV electricity sold)

This also implies that in a policy-scheme where households can sell the renewable energy they generated to the grid in return for a financial remuneration (as opposed to using the grid as a storage medium), the price of PV electricity offered to the households will have to be above 0.6 PLN/kWh to promote the installation of rooftop solar PV modules.

6 Business model for accelerating rooftop PV installation

Figure 6.1 shows the investments that have to be made by the residents of Kalwaria Zebrzydowska (at the optimum houses as suggested by the GAMS model output) at different retail prices of grid electricity. Evidently, the capital to be spent is large and hence might deter residents from installing rooftop PV modules.

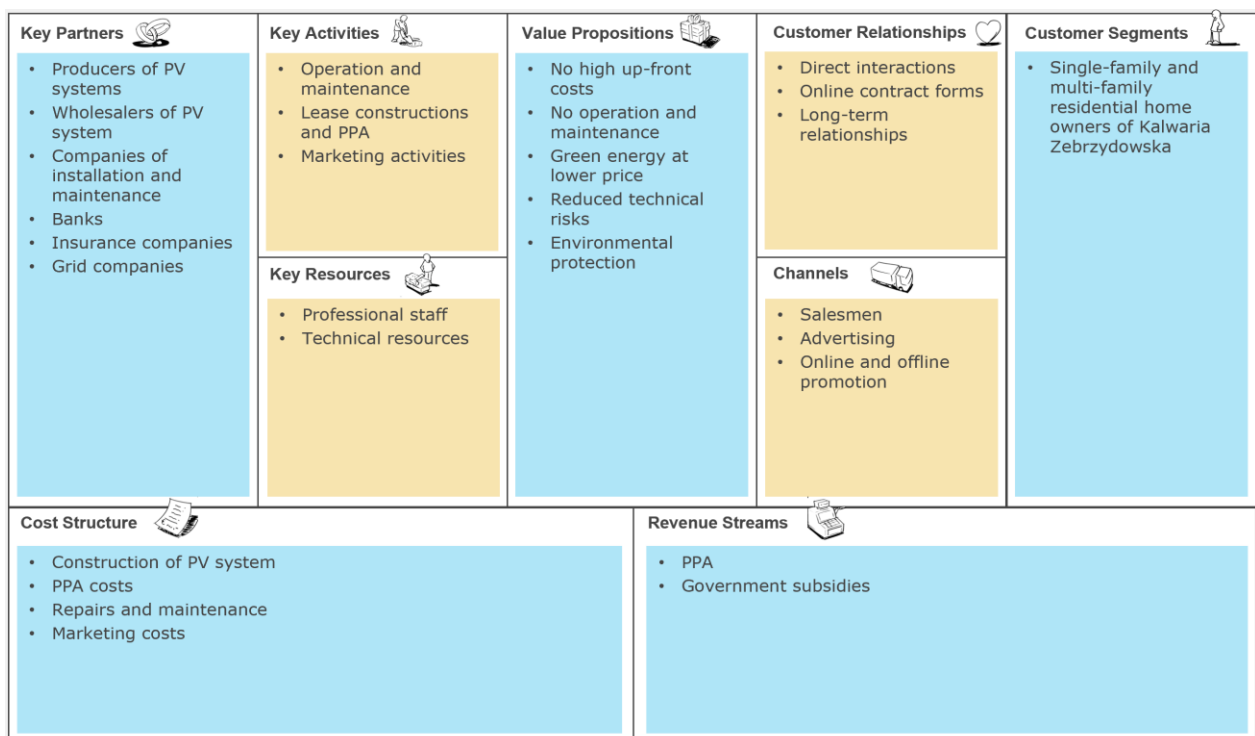


[source: own study]

Figure 6.1: Cost of installing rooftop solar PV modules in optimum roofs (as found through the GAMS model) in Kalwaria with respect to the retail price of electricity

Therefore, the feasibility of a third-party-owned (TPO) business model was examined. In the TPO model, the infrastructure of the rooftop solar PV modules will be owned by a third-party. The business model relies on the hypotheses (1) that all 1090 households, of Kalwaria Zebrzydowska, studied in the project are already willing to provide their roofs for installing the PV modules and hence marketing costs will be ignored in the business model (2) all the energy generated annually will be sold to the customer. Once the electricity is bought by the customers, it is their choice whether they will consume it or use the grid as a storage medium to store the energy for future consumption (as per the grid-storage scheme mentioned in section 4.3).

The business model canvas has been presented in Figure 6.2. Besides removing the burden of high up-front costs of installing the PV modules, the TPO model also ensures that the maintenance and repair of the modules are also managed by the third-party. Furthermore, the renewable electricity that is generated can be bought by the owner of the house/roof at a price that is 30-50% of the retail price of electricity in the grid. The main customer segment in this project is comprised of the owners of single-family and multi-family houses in the city of Kalwaria Zebrzydowska.



(Source: Cai *et al.*, 2019)

Figure 6.2: TPO business model canvas

Channels to reach out to customers will be through salesmen, online and offline promotions. However, since the BMC has been based on the hypothesis that all households are already willing to provide their roofs for PV installations, the role of these channels will be minimal. However, these customers will have to be retained for long periods of time since power purchase agreements (PPA) are signed for 10-25 years. The duration of this venture is assumed to be 25 years. So, customer relations have to be ensured through consulting services for customers at in-person and online platforms.

The key activities of this venture will be collecting revenue through the PPA and maintaining and enhancing customer relations. The third-party should

also ensure stable operation of the PV systems and provide sufficient and uninterrupted power supply. The key partners that make the venture possible will be the wholesalers and manufacturers of PV systems, banks, grid companies and insurance companies to lessen the risk of co-operation between the third-party companies and customers.

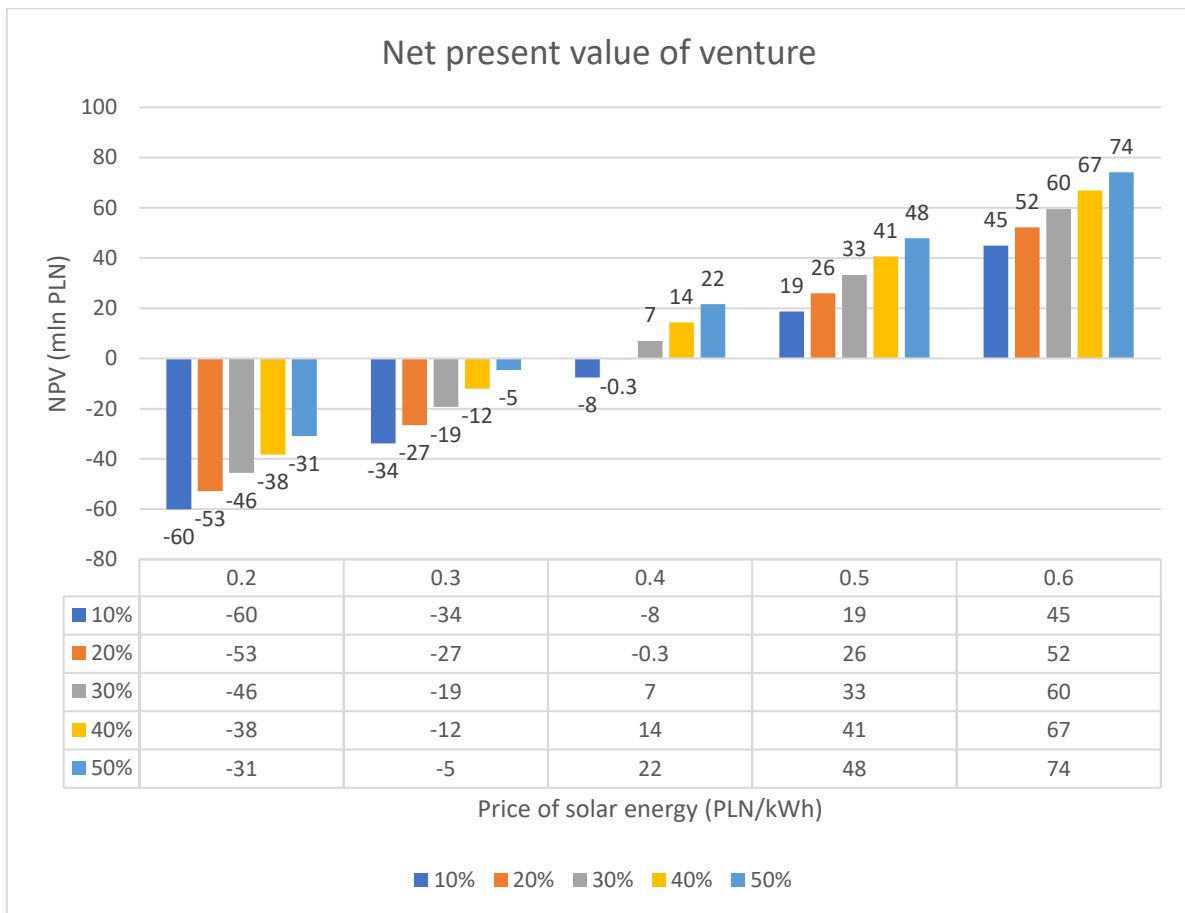
The key resources required are professional staff and abundant technical resources. The staff needs to maintain good relations with the local residents' association to help conduct business activities with the residential area, with the government to procure any subsidies that can be availed, and with the banks to get sufficient loans.

The major costs incurred are the capital costs of PV module instalment, maintenance and repair and the wages paid to the employees that conduct the operations and maintenance. The revenue stream will be the fee paid by the customers for each unit of renewable energy generated. To examine if the revenue and costs accumulated over 25 years would allow the business to be feasible, a financial model was created to calculate the NPV of the venture. The CAPEX and OPEX was calculated using the installation costs and maintenance fees mentioned in section 4.3. The discounting and inflation rates used were also the same. The variables in the financial model of the business model were the value of the subsidies provided by the government (as a percentage of the capital costs) and the price per kWh of solar energy purchased by the customer as agreed by the PPA. The calculations have been presented in Appendix II to show how the math was performed.

Thus, a sensitivity analysis was conducted on the NPV by varying the price of solar energy and subsidy rate on the capital costs. The price was varied from 0.2 to 0.6 PLN/kWh and the rate of subsidy was varied from 10-50% of the capital costs. The results have been tabulated in Figure 6.3.

The x-axis shows the price of solar energy, and the y-axis shows the NPV. It can be seen that the venture is not profitable unless the price of solar energy is between 0.4-0.5 PLN/kWh and the capital costs are subsidised by 20-30%. However, the standard prices of solar energy from rooftop PV modules should be 0.25-0.35 PLN/kWh. Even at prices as high as 0.4-0.5 PLN/kWh, the venture is only able to break even within 25 years. Even if the subsidies go to as high as

50%, the venture is only able to make 22 million PLN at the end of 25 years. Therefore, in the best interest of the society, the venture could be made a public enterprise as opposed to a private one so that the urgency of making profits are reduced.



[source: own study]

Figure 6.3: Sensitivity analysis of the NPV of the venture with respect to the price of solar energy and government subsidies

7 Conclusions

By integrating a wide variety of energy saving techniques and diverse technologies, energy demands in urban buildings can be reduced and met in a cost-effective way. This study focused on retrofitting of the residential buildings in Kalwaria Zebrzydowska to reduce their space heating demands. The retrofitting measures that were analysed here are replacement of windows, modification of roofs and walls to provide better insulation, upgrading of heating technology and installation of rooftop solar PV modules. The entirety of the study was assisted by the geo-referencing of building specific data using a GIS platform called QGIS. This allowed for the energy-analyses of each building.

The feasibility of installing rooftop solar PV modules necessitated the estimation of annual solar radiation on the roofs of the residential buildings in Kalwaria. Two methods were employed to estimate the solar PV output (and thus a solar cadastre for Kalwaria Zebrzydowska's residential buildings)—(1) using regression model of solar radiation using data from PVGIS and (2) using solar radiation model of SAGA GIS. Method 2 produced a more accurate and reliable solar cadastre. It also yielded data about the peak power of the PV modules that can be installed on each roof whereas method 1 only yielded a solar cadastre. It was found that it is feasible to install 16.16 MWp worth of NU-JC370 PV modules in the city, which can generate 18.64 GWh of PV electricity annually.

Every family in Poland requires approximately 5-6 kWp of electricity which can be generated by 14 NU-JC370 PV modules. And this study showed that 91% of the single-family households in Kalwaria Zebrzydowska are capable of hosting more than 15 PV modules. However, most of the solar energy is available only in the summer. Therefore, the policy scheme that allows Polish households to use the electricity grid as a storage medium for renewable energy that they generated, so that they can reclaim (85% of) that energy when required, say in winter, is resourceful.

The estimate of the peak power that can be installed on each roof enabled the estimation of the CAPEX and OPEX that would be borne out of their PV installations. The estimate of the electricity generated helped to calculate the

money that can be saved through the free electricity received. Implementation of retrofit measure will further reduce the energy demands in the homes as well.

However, until the price of electricity reaches 0.6 PLN/kWh, it is not financially ideal to install rooftop PV modules on any roofs. Below 0.6 PLN/kWh, the optimum solution would be to implement only thermo-modernisation and upgrade of heating technology. This optimum solution would require an investment of 87.43 million PLN which includes the cost of thermo-modernisation, upgrade of heating technology and fuel costs for 15 years, with 81% of the households using high efficiency hard coal-boilers of 14 kW capacity. Without any changes, that is, in the initial scenario the heating technology was comprised of low efficiency hard coal-boiler of capacity 19 kW (40%) and 25 kW (40%) –clearly indicating that the heating systems were oversized prior to thermo-modernisation and upgrade of heating technologies.

However, when the price of electricity is above 0.6 PLN/kWh, rooftop solar PV becomes feasible; the money saved by reclaiming the PV electricity stored in the grid reduces the total cost of retrofitting from 87.43 mln PLN when electricity price is 0.6 PLN/kWh to 30.67 mln PLN when the electricity price is 1 PLN/kWh.

Installation of rooftop PV modules, however, consumes heavy capital which is unlikely to be borne by the owner of every house. Therefore, a third-party-owned business model is proposed. However, in 25 years, the venture will not break even until the price of solar energy paid to the third-part by the customers in 0.4 PLN/kWh (which is higher than the norm) and the capital costs are subsidised by 20-30%. In fact, the NPV of the venture reaches only 22 million PLN at a price of 0.4 PLN/kWh and subsidy of 50%. Hence the business is not very lucrative. Therefore, in the best interest of the society, the venture should be a public entity rather than a private one.

8 Nomenclature

A^f	Total heated area of the building [m^2]
A^z	Building area on the outer contour of the building [m^2]
c^f	Heated area calibration ratio
d	Annual demolishing rate of existing heated area [%]
e^u	Specific heat demand for energy service 'u' in buildings per area [$kWh/(m^2 \cdot year)$]
l	Number of floors above ground level
Q^u	Useful heat demand for energy service u [$kWh/year$]
r	Remaining building area after modernisation and demolishing [%]
y	Number of years after the base year
α	Annual thermo-modernisation rate of the existing buildings area by classes [%]
ϵ	Annual energy intensity improvement due to thermo-modernisation
b	Building belonging to set B
cl	Class of heat intensity within a building type belonging to set CL
k	Grid cell belonging to set k
new	New construction after the base year 2015
s	Balance zone belonging to set S
t	Building utility type belonging to set T
u	Energy service including space heating (h), ventilation (ve) and domestic hot water preparation (w)

9 References

- Agugiaro, G. *et al.* (2012) 'Solar radiation estimation on building roofs and web-based solar cadaster', *ISPRS Annals of the Photogrammetry, Remote Sensing and Spatial Information Sciences*, 1(September), pp. 177–182. doi: 10.5194/isprsannals-I-2-177-2012.
- Anastaselos, D., Oxizidis, S. and Papadopoulos, A. M. (2011) 'Energy, environmental and economic optimization of thermal insulation solutions by means of an integrated decision support system', *Energy and Buildings*, 43(2–3), pp. 686–694. doi: 10.1016/j.enbuild.2010.11.013.
- Böhner, J. and Antonić, O. (2009) 'Land-surface parameters specific to topo-climatology', in *Developments in soil science*, pp. 195–226. doi: 10.1016/S0166-2481(08)00008-1.
- Cai, X. *et al.* (2019) 'Business models of distributed solar photovoltaic power of China: The Business Model Canvas perspective', *Sustainability (Switzerland)*, 11(16). doi: 10.3390/su11164322.
- European Commission (2017) *JRC Photovoltaic Geographical Information System (PVGIS) - European Commission, Photovoltaic Geographical Information System*. Available at: https://re.jrc.ec.europa.eu/pvg_tools/es/#TMY (Accessed: 15 December 2020).
- Fioretti, R. *et al.* (2010) 'Green roof energy and water related performance in the Mediterranean climate', *Building and Environment*, 45(8), pp. 1890–1904. doi: 10.1016/j.buildenv.2010.03.001.
- Hong, T. *et al.* (2017) 'Development of a method for estimating the rooftop solar photovoltaic (PV) potential by analyzing the available rooftop area using Hillshade analysis', *Applied Energy*, 194, pp. 320–332. doi: 10.1016/j.apenergy.2016.07.001.
- IEE Project TABULA (2012) *IEE Project TABULA*. Available at: <https://episcope.eu/iee-project/tabula/>.
- Jing, R. *et al.* (2020) 'Quantifying the contribution of individual technologies in integrated urban energy systems – A system value approach', *Applied Energy*, 266(March), p. 114859. doi: 10.1016/j.apenergy.2020.114859.
- Jurasz, J. K., Dąbek, P. B. and Campana, P. E. (2020) 'Can a city reach energy self-sufficiency by means of rooftop photovoltaics? Case study from Poland', *Journal of Cleaner Production*, 245. doi: 10.1016/j.jclepro.2019.118813.
- Kereush, D. and Perovych, I. (2017) 'Determining Criteria for Optimal Site Selection for Solar Power Plants', *Geomatics, Landmanagement and Landscape*, 4(4), pp. 39–54. doi: 10.15576/gll/2017.4.39.
- Kim, K. H., Kabir, E. and Kabir, S. (2015) 'A review on the human health impact of airborne particulate matter', *Environment International*, 74, pp. 136–143. doi:

10.1016/j.envint.2014.10.005.

Lindberg, F. *et al.* (2015) 'Solar energy on building envelopes - 3D modelling in a 2D environment', *Solar Energy*, 115, pp. 320–332. doi: 10.1016/j.apenergy.2016.07.001.

Luković, J. B. *et al.* (2015) 'High resolution grid of potential incoming solar radiation for Serbia', *Thermal Science*, 19, pp. S427–S435. doi: 10.2298/TSCI150430134L.

Mahmoud, R. M. *et al.* (2019) 'Estimation of load duration curves from general building data in the building stock using dynamic BES-models', *E3S Web of Conferences*, 111(201 9). doi: 10.1051/e3sconf/201911101078.

Mastrucci, A. *et al.* (2014) 'Estimating energy savings for the residential building stock of an entire city: A GIS-based statistical downscaling approach applied to Rotterdam', *Energy and Buildings*, 75, pp. 358–367. doi: 10.1016/j.enbuild.2014.02.032.

Peters, A. *et al.* (2000) 'Associations between mortality and air pollution in central Europe', *Environmental Health Perspectives*, 108(4), pp. 283–287. doi: 10.1289/ehp.00108283.

Shi, X. (2011) 'Design optimization of insulation usage and space conditioning load using energy simulation and genetic algorithm', *Energy*, 36(3), pp. 1659–1667. doi: 10.1016/j.energy.2010.12.064.

Šúri, M. *et al.* (2007) 'Potential of solar electricity generation in the European Union member states and candidate countries', *Solar Energy*, 81(10), pp. 1295–1305. doi: 10.1016/j.solener.2006.12.007.

Theodoridou, I. *et al.* (2012) 'Assessment of retrofitting measures and solar systems' potential in urban areas using Geographical Information Systems: Application to a Mediterranean city', *Renewable and Sustainable Energy Reviews*, 16(8), pp. 6239–6261. doi: 10.1016/j.rser.2012.03.075.

Wyrwa, A. (2019) 'City-level energy planning aimed at emission reduction in residential sector with the use of decision support model and geodata', *IOP Conference Series: Earth and Environmental Science*, 214(1). doi: 10.1088/1755-1315/214/1/012039.

Wyrwa, A. and Chen, Y. K. (2017) 'Mapping urban heat demand with the use of gis-based tools', *Energies*, 10(5). doi: 10.3390/en10050720.

Agugiaro, G. *et al.* (2012) 'Solar radiation estimation on building roofs and web-based solar cadaster', *ISPRS Annals of the Photogrammetry, Remote Sensing and Spatial Information Sciences*, 1(September), pp. 177–182. doi: 10.5194/isprsannals-I-2-177-2012.

Anastaselos, D., Oxizidis, S. and Papadopoulos, A. M. (2011) 'Energy,

environmental and economic optimization of thermal insulation solutions by means of an integrated decision support system', *Energy and Buildings*, 43(2–3), pp. 686–694. doi: 10.1016/j.enbuild.2010.11.013.

Böhner, J. and Antonić, O. (2009) 'Land-surface parameters specific to topoclimatology', in *Developments in soil science*, pp. 195–226. doi: 10.1016/S0166-2481(08)00008-1.

Cai, X. *et al.* (2019) 'Business models of distributed solar photovoltaic power of China: The Business Model Canvas perspective', *Sustainability (Switzerland)*, 11(16). doi: 10.3390/su11164322.

European Commission (2017) *JRC Photovoltaic Geographical Information System (PVGIS) - European Commission, Photovoltaic Geographical Information System*. Available at: https://re.jrc.ec.europa.eu/pvg_tools/es/#TMY (Accessed: 15 December 2020).

Fioretti, R. *et al.* (2010) 'Green roof energy and water related performance in the Mediterranean climate', *Building and Environment*, 45(8), pp. 1890–1904. doi: 10.1016/j.buildenv.2010.03.001.

Hong, T. *et al.* (2017) 'Development of a method for estimating the rooftop solar photovoltaic (PV) potential by analyzing the available rooftop area using Hillshade analysis', *Applied Energy*, 194, pp. 320–332. doi: 10.1016/j.apenergy.2016.07.001.

IEE Project TABULA (2012) *IEE Project TABULA*. Available at: <https://episcopus.eu/iee-project/tabula/>.

Jing, R. *et al.* (2020) 'Quantifying the contribution of individual technologies in integrated urban energy systems – A system value approach', *Applied Energy*, 266(March), p. 114859. doi: 10.1016/j.apenergy.2020.114859.

Jurasz, J. K., Dąbek, P. B. and Campana, P. E. (2020) 'Can a city reach energy self-sufficiency by means of rooftop photovoltaics? Case study from Poland', *Journal of Cleaner Production*, 245. doi: 10.1016/j.jclepro.2019.118813.

Kereush, D. and Perovych, I. (2017) 'Determining Criteria for Optimal Site Selection for Solar Power Plants', *Geomatics, Landmanagement and Landscape*, 4(4), pp. 39–54. doi: 10.15576/gll/2017.4.39.

Kim, K. H., Kabir, E. and Kabir, S. (2015) 'A review on the human health impact of airborne particulate matter', *Environment International*, 74, pp. 136–143. doi: 10.1016/j.envint.2014.10.005.

Lindberg, F. *et al.* (2015) 'Solar energy on building envelopes - 3D modelling in a 2D environment', *Solar Energy*, 115, pp. 320–332. doi: 10.1016/j.apenergy.2016.07.001.

Luković, J. B. *et al.* (2015) 'High resolution grid of potential incoming solar radiation for Serbia', *Thermal Science*, 19, pp. S427–S435. doi: 10.2298/TSCI150430134L.

Mahmoud, R. M. *et al.* (2019) 'Estimation of load duration curves from general building data in the building stock using dynamic BES-models', *E3S Web of Conferences*, 111(2019), pp. 1–9. doi: 10.1051/e3sconf/201911101078.

Mastrucci, A. *et al.* (2014) 'Estimating energy savings for the residential building stock of an entire city: A GIS-based statistical downscaling approach applied to Rotterdam', *Energy and Buildings*, 75, pp. 358–367. doi: 10.1016/j.enbuild.2014.02.032.

Peters, A. *et al.* (2000) 'Associations between mortality and air pollution in central Europe', *Environmental Health Perspectives*, 108(4), pp. 283–287. doi: 10.1289/ehp.00108283.

Shi, X. (2011) 'Design optimization of insulation usage and space conditioning load using energy simulation and genetic algorithm', *Energy*, 36(3), pp. 1659–1667. doi: 10.1016/j.energy.2010.12.064.

Šúri, M. *et al.* (2007) 'Potential of solar electricity generation in the European Union member states and candidate countries', *Solar Energy*, 81(10), pp. 1295–1305. doi: 10.1016/j.solener.2006.12.007.

Theodoridou, I. *et al.* (2012) 'Assessment of retrofitting measures and solar systems' potential in urban areas using Geographical Information Systems: Application to a Mediterranean city', *Renewable and Sustainable Energy Reviews*, 16(8), pp. 6239–6261. doi: 10.1016/j.rser.2012.03.075.

Wyrwa, A. (2019) 'City-level energy planning aimed at emission reduction in residential sector with the use of decision support model and geodata', *IOP*

Conference Series: Earth and Environmental Science, 214(1). doi:
10.1088/1755-1315/214/1/012039.

Wyrwa, A. and Chen, Y. K. (2017) 'Mapping urban heat demand with the use of
gis-based tools', *Energies*, 10(5). doi: 10.3390/en10050720.

Appendix I

GAMS ID	QGIS ID	Area available on suitable roofs (m2)	Number of modules that can be fitted on the roof top	Peak power on each roof (kWp)	Total PV Output (kWh/year) [Method 2]	Total revenue [PLN]	CAPEX [PLN]	OPEX [PLN] total	Total cost [PLN]
1	3523	51	24	8.88	10403.85857	55074.13	39960	19163.04	59123.04
2	3181	47	22	8.14	9683.002561	51258.19	36630	17566.12	54196.12
3	5206	81	39	14.43	16371.97275	86667.09	64935	31139.93	96074.93
4	3652	94	45	16.65	19692.6254	104245.39	74925	35930.69	110855.7
5	3182	71	34	12.58	15178.1048	80347.20	56610	27147.64	83757.64
6	3134	49	23	8.51	10611.28034	56172.15	38295	18364.58	56659.58
7	3137	28	13	4.81	4837.515937	25608.00	21645	10379.98	32024.98
8	2912	61	29	10.73	13180.41134	69772.16	48285	23155.34	71440.34
9	3115	45	21	7.77	7586.318398	40159.13	34965	16767.66	51732.66
10	5418	29	14	5.18	4998.188362	26458.54	23310	11178.44	34488.44
11	3106	135	65	24.05	30734.58607	162697.39	108225	51899.89	160124.9
12	2741	3	1	0.37	341.8662469	1809.71	1665	1996.15	3661.15
13	3421	9	4	1.48	1372.481893	7265.41	6660	7984.599	14644.6
14	3093	15	7	2.59	2454.71926	12994.36	11655	5589.219	17244.22
15	5174	54	26	9.62	12877.26607	68167.43	43290	20759.96	64049.96
16	3435	78	37	13.69	17096.82494	90504.19	61605	29543.01	91148.01
17	3640	93	45	16.65	19122.86085	101229.27	74925	35930.69	110855.7
18	3407	36	17	6.29	7095.816383	37562.60	28305	13573.82	41878.82
19	2797	93	45	16.65	19065.88611	100927.66	74925	35930.69	110855.7
20	3122	84	40	14.80	17266.70391	91403.47	66600	31938.39	98538.39

Appendix II

Year #	Revenue (mln PLN)	Costs (mln PLN)	Discounting factor	Inflation factor	Present value (mln PLN)	Cumulative present value (mln PLN)
0	0	36.3694275	1.000	1.000	-36.3694275	-36.3694275
1	7.45	2.68794828	0.952	1.020	4.487555803	-31.8818717
2	7.45	2.68794828	0.907	1.040	4.224126484	-27.65774521
3	7.45	2.68794828	0.864	1.061	3.974662451	-23.68308276
4	7.45	2.68794828	0.823	1.082	3.738458092	-19.94462467
5	7.45	2.68794828	0.784	1.104	3.514842551	-16.42978212
6	7.45	2.68794828	0.746	1.126	3.303178047	-13.12660407
7	7.45	2.68794828	0.711	1.149	3.102858264	-10.02374581
8	7.45	2.68794828	0.677	1.172	2.91330682	-7.110438988
9	7.45	2.68794828	0.645	1.195	2.733975816	-4.376463172
10	7.45	2.68794828	0.614	1.219	2.564344443	-1.812118729
11	7.45	2.68794828	0.585	1.243	2.403917671	0.591798942
12	7.45	2.68794828	0.557	1.268	2.252224986	2.844023928
13	7.45	2.68794828	0.530	1.294	2.108819204	4.952843132
14	7.45	2.68794828	0.505	1.319	1.973275324	6.926118456
15	7.45	2.68794828	0.481	1.346	1.845189455	8.771307911
16	7.45	2.68794828	0.458	1.373	1.724177782	10.49548569
17	7.45	2.68794828	0.436	1.400	1.609875583	12.10536128
18	7.45	2.68794828	0.416	1.428	1.501936303	13.60729758
19	7.45	2.68794828	0.396	1.457	1.400030662	15.00732824
20	7.45	2.68794828	0.377	1.486	1.303845809	16.31117405
21	7.45	2.68794828	0.359	1.516	1.213084522	17.52425857
22	7.45	2.68794828	0.342	1.546	1.127464442	18.65172301
23	7.45	2.68794828	0.326	1.577	1.04671734	19.69844035
24	7.45	2.68794828	0.310	1.608	0.970588434	20.66902879
25	7.45	2.68794828	0.295	1.641	0.89883572	21.56786451
					NPV	21.56786451